

Supplementary material for

Modifying the terminal phenyl group of monomethine cyanine dyes as a pathway to brighter nucleic acid probes

Johanna M. Alaranta, Arto M. Valkonen, Sailee S. Shroff, Varpu S. Marjomäki, Kari Rissanen and Tanja M. Lahtinen*

Table of Contents

1. Experimental Procedures	2
2. Synthesis Procedures	2
2.1. General synthesis procedure for the quinolines	2
2.2. General method for the dye synthesis	5
3. NMR Spectra	8
4. X-ray Diffraction	15
5. Computational Studies	18
5.1 General	18
5.2 The Cartesian Coordinates	18
6. UV-vis Spectra.....	22
7. Fluorescence Spectra	25
8. Literature.....	30

1. Experimental Procedures

All reagents were used as purchased apart from 1,2-dichloroethane which was distilled and stored in fridge under 3 Å molecular sieves. K₂CO₃ was dried at 120 °C overnight to make sure it was anhydrous. NMR spectra were measured with Bruker Avance III 500 MHz NMR spectrometer. Accurate MS spectra were measured with Agilent 6560 LC-IMMS-TOF mass spectrometer.

Spectroscopy measurements were done in room temperature with Hellma 110-QS-absorption cuvettes or 111-QS-fluorescence cuvettes with 10 mm light path. pH was kept at constant 7.6 in TE buffer and nucleic acid solutions. Calf thymus (ct) DNA was purchased from Sigma-Aldrich and stored in fridge. Ethanol was chosen as an organic solvent to investigate the absorption coefficient to ensure stable dye concentration by choosing a solvent with higher boiling point than previously used DCM.¹ Ethanol is also used to extract the SYBR Green I from DNA after imaging is completed.² Absorption spectra were measured with Perkin Elmer 650 UV-vis spectrometer. Varian Cary Eclipse fluorescence spectrometer was used to collect emission and excitation data. Dry DMSO was used to prepare stock solutions of the dyes in 19.6 mM concentration. Viral RNA was extracted as previously described.¹

2. Synthesis Procedures

2.1. General synthesis procedure for the quinolines

Synthesis was performed based on procedure reported by Ying.³ 4-methylcarbostyryl (**6**, 1.0 g, 6.3 mmol), copper powder (**7**, 2.3 g, 36.5 mmol), anhydrous K₂CO₃ (**8**, 0.88 g, 6.3 mmol) and substituted 4-iodobenzene (**9-11**)* were mixed in oven dried flask equipped with reflux condenser and sealed with CaCl₂-tube. Dry DMF (15 ml) was added, and mixture was stirred vigorously to dissolve all compounds. Resulting mixture was heated to 160 °C on an oil bath and stirred overnight. In the morning, mixture was allowed to cool to room temperature and filtered through a pad of Hyflo Super gel. Solvent was evaporated resulting to a black oil. Water and ethyl acetate were introduced to the oil. Mixture was filtered again through a pad of Hyflo Super gel to remove formed solid. After filtering, organic layer was washed with water and brine and dried with Na₂SO₄. Solvent was evaporated and resulting solid was dissolved again in a mixture of 1:4 hexane and ethyl acetate and purified with flash column chromatography using the Hex/EtOAc mixture as eluent.

*Used compounds are listed below for each individual synthesis.

1-(4-(dimethylamino)phenyl)-4-methylquinolin-2(1H)-one (12)

General synthesis route was used to synthesize compound **12** with 4-bromo-*N,N*-dimethylaniline (**9**, 1.88 g, 9.4 mmol). Because starting material had bromine instead of iodine, mixture was heated two days at 160 °C instead of one. Compound was collected as brown solid. Product was used in the next step without further purifications. Yield with small impurities 512.8 mg (1.84 mmol, 28.8 %).

Expected accurate mass $[M+Na]^+$ m/z 301.1311, observed m/z 301.1311.

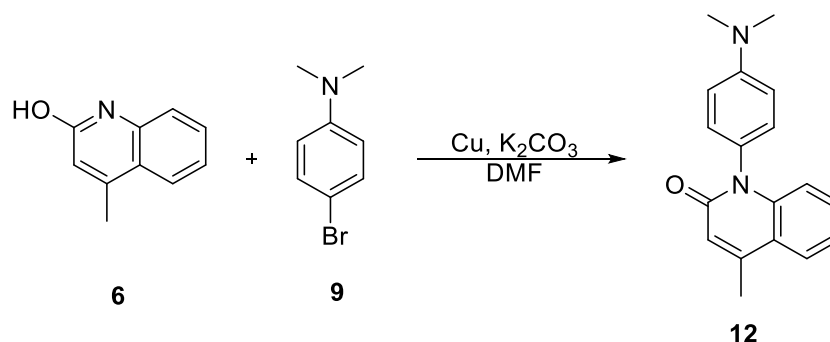


Fig. S1. Synthesis route for quinoline **12**.

1-(4-(2-(2-(2-methoxyethoxy)ethoxy)ethoxy)phenyl)-4-methylquinolin-2(1H)-one (17)

Tosylation of triethylene glycol monomethyl ether (PEG) was performed as described by Nguyen *et al.*⁴ PEG (**13**, 1.724 ml, 10.0 mmol) was dissolved in pyridine (1.724 ml) at 0 °C. *p*-toluenesulfonyl chloride (**14**, 2.2878 g, 12.0 mmol) was dissolved in 3.6 ml of pyridine and added to the reaction mixture. Resulting pale yellow solution was stirred at 0 °C for four hours. After mixing, ice and 25 ml of 6 N HCl was added to the thick orange solution. DCM was introduced to the mixture and the water phase was extracted three times with more DCM. Organic phases were combined and finally washed with 2 N HCl. Resulting organic phase was dried with Na₂SO₄ overnight. Solution was filtered and solvent was evaporated. Product **15** was collected as a pale yellow oil. Yield 3.101 g (9.7 mmol, 97 %) Tosylated PEG (**15**) was used as such without further purification steps.

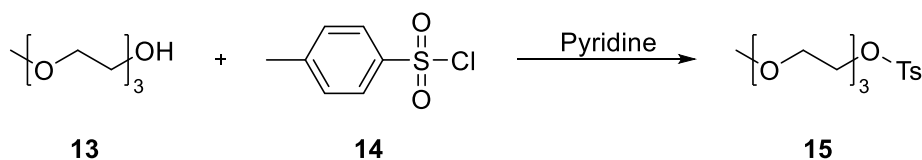


Fig. S2. Tosylation of PEG **13**.

Pegylation of 4-iodophenol was done according to the procedure published by Nguyen *et al.*⁴ 4-iodophenol (**10**, 2.2 g, 10.0 mmol) was dissolved in 70 ml of acetonitrile. Formed light pink solution was heated to 80 °C on an oil bath. To the hot mixture, K₂CO₃ (**8**, 1.6 g, 12.0 mmol) was added. Resulting cloudy mixture was stirred vigorously before adding the tosylated PEG (**15**, 3.1 g, 9.7 mmol). Resulting mixture was refluxed overnight under N₂-atmosphere. In the

morning white solution was allowed to cool to room temperature after which solvent was evaporated under reduced pressure. Water and DCM were introduced to the residue. Aquatic phase was extracted three times with DCM. Organic phases were combined and washed three times with NaOH-solution (pH 12). Organic layer was dried with Na₂SO₄ after which the solvent was evaporated. Desired product was collected as pale yellow oil. Yield 3.18 g (8.7 mmol, 86.8 %). Pegylated 4-iodophenol was used as such in the next step without further purification.

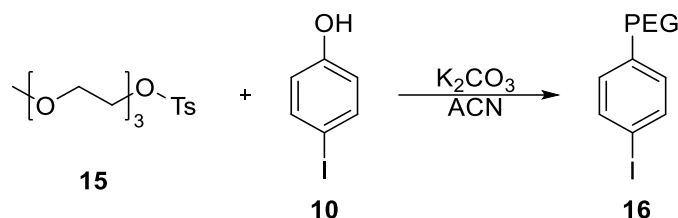


Fig. S3. Pegylation of 4-iodophenol **10**.

Pegylated quinolinone was synthesized accordingly to the general method. Pegylated 4-iodophenol from previous step was used as substituted 4-iodobenzene (**16**, 3.18 g, 8.7 mmol). Column was not needed to purify the compound. After washing with water and drying organic phase, solvent was evaporated, and product was isolated by filtering the residue through cotton. Product **17** was collected as brown oil. Resulted product was used in the next step without further purifications. Yield with small impurities 1.3505 g (3.4 mmol, 54.0 %)

Expected accurate mass [M+H]⁺ m/z 398.1962, observed m/z 398.1967.

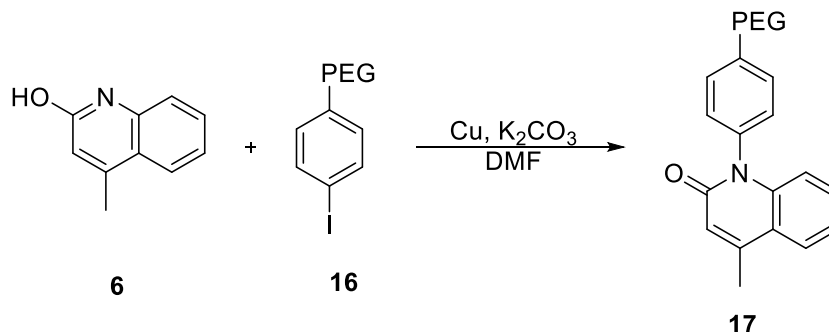


Fig. S4. Synthesis of quinoline **17**.

1-(4-methoxyphenyl)-4-methylquinolin-2(1H)-one, (18)

Compound **18** was synthesized according to the general procedure. 4-iodoanisole (**11**, 2.18 g, 9.3 mmol) was used as substituted 4-iodobenzene. Product was collected as red solid. Intermediate was used in the next step without further purifications. Yield with small impurities 374.6 mg (1.41 mmol, 22.4 %)

Expected accurate mass [M+H]⁺ m/z 266.1176, observed m/z 266.1182.

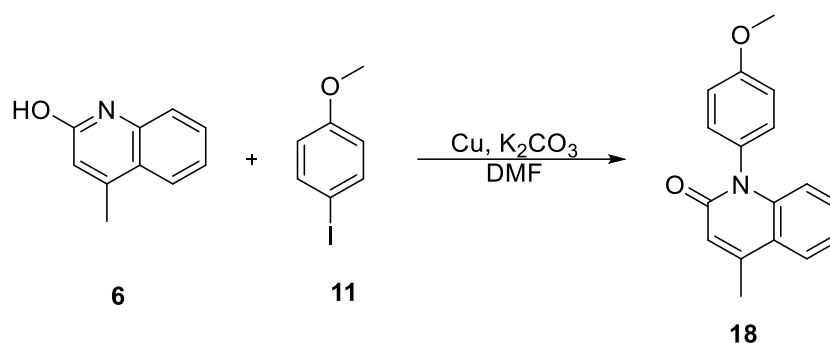


Fig. S5. Synthesis route of quinoline **18**.

2.2. General method for the dye synthesis

Previously synthesized quinoline* (**12**, **17** or **18**, 0.438 mmol) was dissolved in distilled 1,2-DCE in N₂ atmosphere. To the stirred solution, POCl₃ was added (**19**, 123 μl, 1.31 mmol). Resulting mixture was heated to 70 °C on an oil bath and mixed overnight. On the morning, solvent was evaporated and resulting oil (**20**, **21** or **22**) was dissolved again in dry DCM. Oxazolium (**23**, 0.1399 g, 0.438 mmol) was prepared as described previously¹ and added to the stirred solution under N₂ atmosphere. Resulting mixture was stirred at room temperature for four hours. After that, solvent was evaporated and resulting oil was purified with flash column chromatography using 10 % MeOH/DCM as eluent. Eluent was evaporated from the fractions containing product. Resulting oil was dissolved in acetonitrile and excess HNMe₂ (5 ml) was added to stirred solution. Resulting mixture was stirred overnight. Water and DCM was added to the solution and aquatic phase was extracted three times with DCM. Organic phases were combined, dried with Na₂SO₄ and finally solvent was evaporated. Product was collected from flash column chromatography using 10 % MeOH/DCM as eluent.

*Synthesis reported above for compounds **12**, **17** and **18**.

2-((2-(dimethylamino)-1-(4-(dimethylamino)phenyl)quinolin-4-ylidene)methyl)-3-methylbenzoxazol-3-ium, (**1**), OxN-NMe₂

Quinoline **12** (0.438 mmol, 0.122 g) was used to synthesize OxN-NMe₂ **1** according to the general method. Product was collected as orange oil. Yield 35.6 mg (0.075 mmol, 12.9 %).

Expected accurate mass [M]⁺ m/z 437.2336, observed 437.2337.

¹H NMR (500 MHz, MeOD) δ 8.44 (dt, *J* = 8.3, 1.7 Hz, 1H), 7.74 (d, *J* = 1.5 Hz, 1H), 7.62 – 7.57 (m, 2H), 7.52 (ddd, *J* = 8.1, 7.0, 1.2 Hz, 1H), 7.41 (d, *J* = 1.0 Hz, 1H), 7.39 (s, 1H), 7.34 – 7.29 (m, 2H), 7.25 (s, 1H), 7.23 (s, 1H), 6.97 (s, 1H), 6.96 (s, 1H), 5.89 (s, 1H), 3.74 (s, 3H), 3.09 (s, 6H), 2.95 (s, 6H).

¹³C NMR (126 MHz, MeOD) δ 161.36, 158.43, 151.02, 149.15, 146.44, 141.18, 131.64, 129.71, 126.31, 125.45, 124.91, 124.54, 123.14, 121.08, 118.31, 112.37, 109.83, 109.00, 101.28, 70.03, 41.91, 39.09, 29.00.

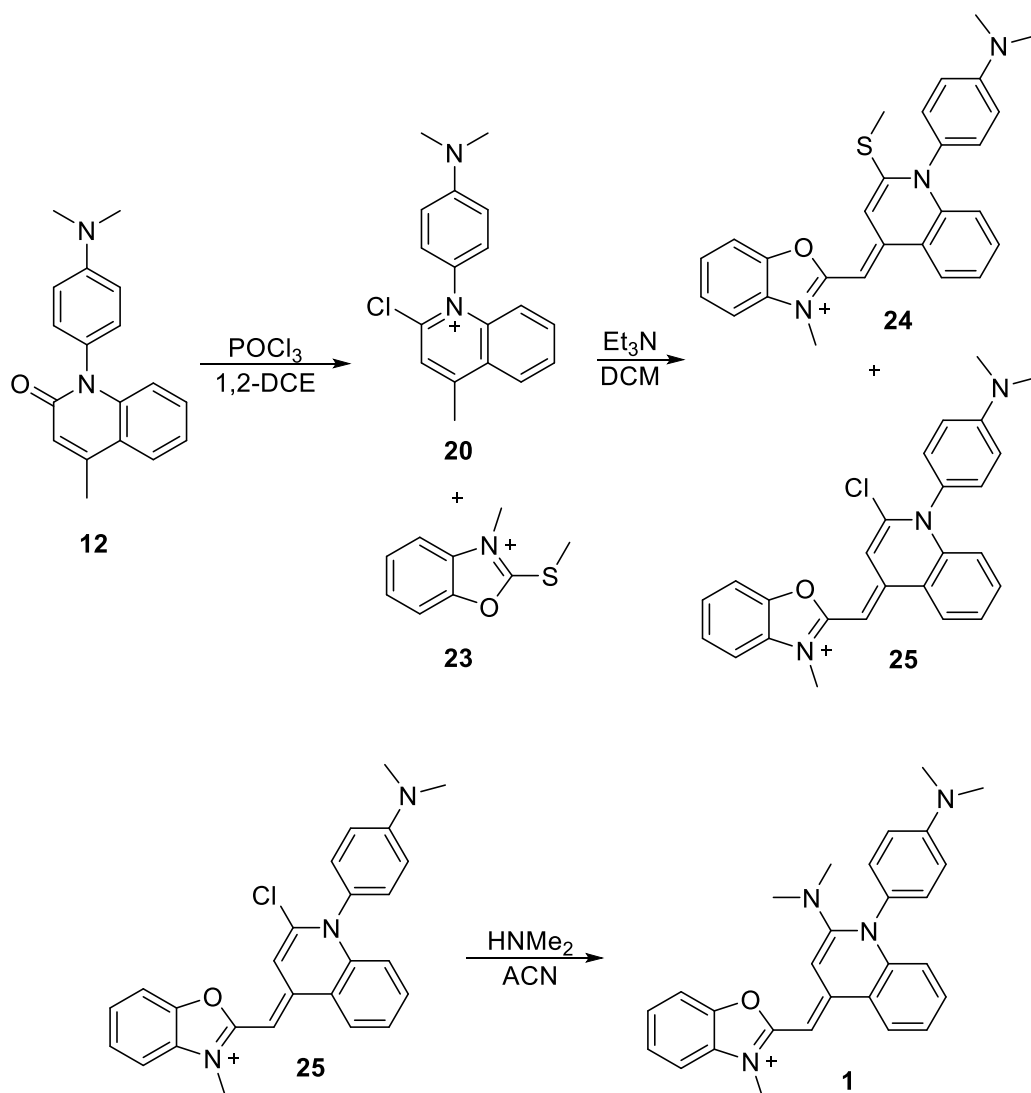


Fig. S6. Synthesis route for dye OxN-NMe₂ 1.

2-((2-(dimethylamino)-1-(4-(2-(2-(2-methoxyethoxy)ethoxy)ethoxy)phenyl)quinolin-4-ylidene)methyl)-3-methylbenzoxazol-3-ium, (**2**), OxN-PEG

Pegylated quinoline **17** (0.438 mmol, 175 μ l) was used in this synthesis, otherwise following the general method. Product was collected as orange oil. Yield 33.5 mg (0.057 mmol, 17.2 %)

Expected accurate mass [M]⁺ m/z 556.2806, observed 556.2809.

¹H NMR (500 MHz, MeOD) δ 8.47 (dd, $J = 8.4, 1.5$ Hz, 1H), 7.76 (s, 1H), 7.63 – 7.59 (m, 2H), 7.54 (ddd, $J = 8.2, 7.0, 1.2$ Hz, 1H), 7.43 (s, 1H), 7.42 (s, 1H), 7.41 (d, $J = 3.7$ Hz, 2H), 7.31 (ddd, $J = 8.5, 5.1, 3.7$ Hz, 1H), 7.28 (d, $J = 1.1$ Hz, 1H), 7.27 (d, $J = 2.6$ Hz, 1H), 7.25 (d, $J = 2.1$ Hz, 1H), 5.94 (s, 1H), 4.29 – 4.26 (m, 2H), 3.93 – 3.90 (m, 2H), 3.77 (s, 3H), 3.76 – 3.73 (m, 2H), 3.70 – 3.67 (m, 2H), 3.67 – 3.65 (m, 2H), 3.57 – 3.54 (m, 2H), 3.36 (s, 3H), 2.94 (s, 6H).

^{13}C NMR (126 MHz, MeOD) δ 163.10, 161.36, 160.02, 151.14, 148.01, 142.29, 133.35, 133.20, 132.78, 132.19, 127.09, 126.60, 126.22, 124.87, 122.68, 119.67, 117.39, 111.46, 110.70, 102.73, 73.14, 72.02, 71.96, 71.77, 71.57, 70.86, 69.39, 59.25, 43.44, 30.63.

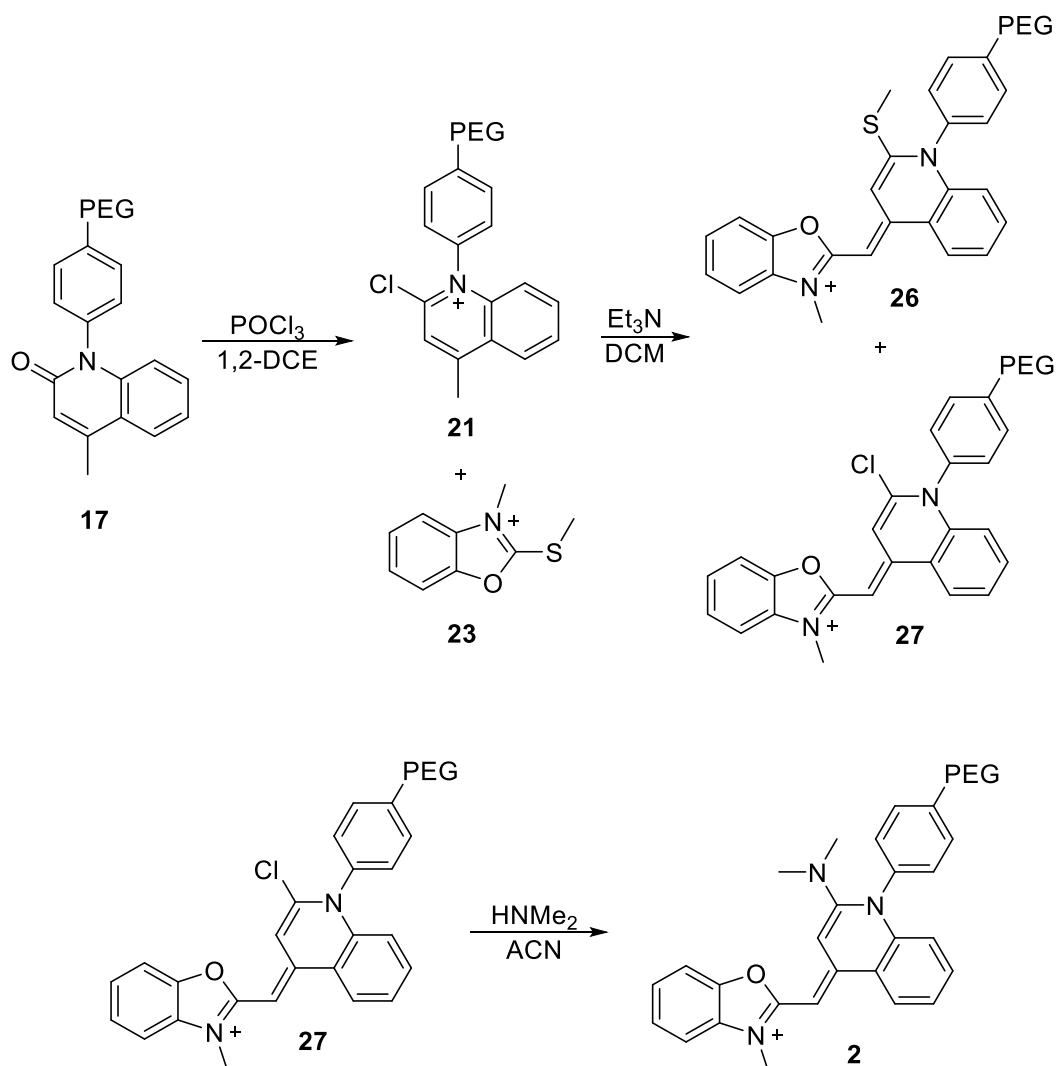


Fig. S7. Synthesis route for dye OxN-PEG **2**.

2-((2-(dimethylamino)-1-(4-methoxyphenyl)quinolin-4-ylidene)methyl)-3-methylbenzoxazol-3-ium, (**3**), OxN-OMe

General method was followed to synthesize OxN-OMe **3** using quinoline **18** (0.483 mmol, 0.1161 g). Product was collected as orange oil. Yield 24.0 mg (0.052 mmol, 11.9 %).

Expected accurate mass $[\text{M}]^+$ m/z 424.2020, observed 424.2027.

^1H NMR (500 MHz, CD_2Cl_2) δ 8.50 – 8.43 (m, 1H), 7.70 (s, 1H), 7.60 – 7.53 (m, 2H), 7.53 – 7.50 (m, 1H), 7.44 – 7.40 (m, 1H), 7.34 – 7.33 (m, 1H), 7.32 (d, $J = 4.3$ Hz, 1H), 7.31 (s, 1H), 7.30 (s, 1H), 7.24 – 7.22 (m, 1H), 7.20 – 7.15 (m, 2H), 5.90 (s, 1H), 3.93 (s, 3H), 3.82 (s, 3H), 2.92 (s, 6H).

^{13}C NMR (126 MHz, CD_2Cl_2) δ 161.91, 161.03, 158.76, 150.17, 146.93, 141.21, 132.75, 132.18, 131.22, 131.07, 128.72, 126.41, 126.07, 125.67, 124.19, 121.71, 118.86, 116.17, 110.82, 109.89, 101.94, 71.78, 56.38, 43.46, 31.20.

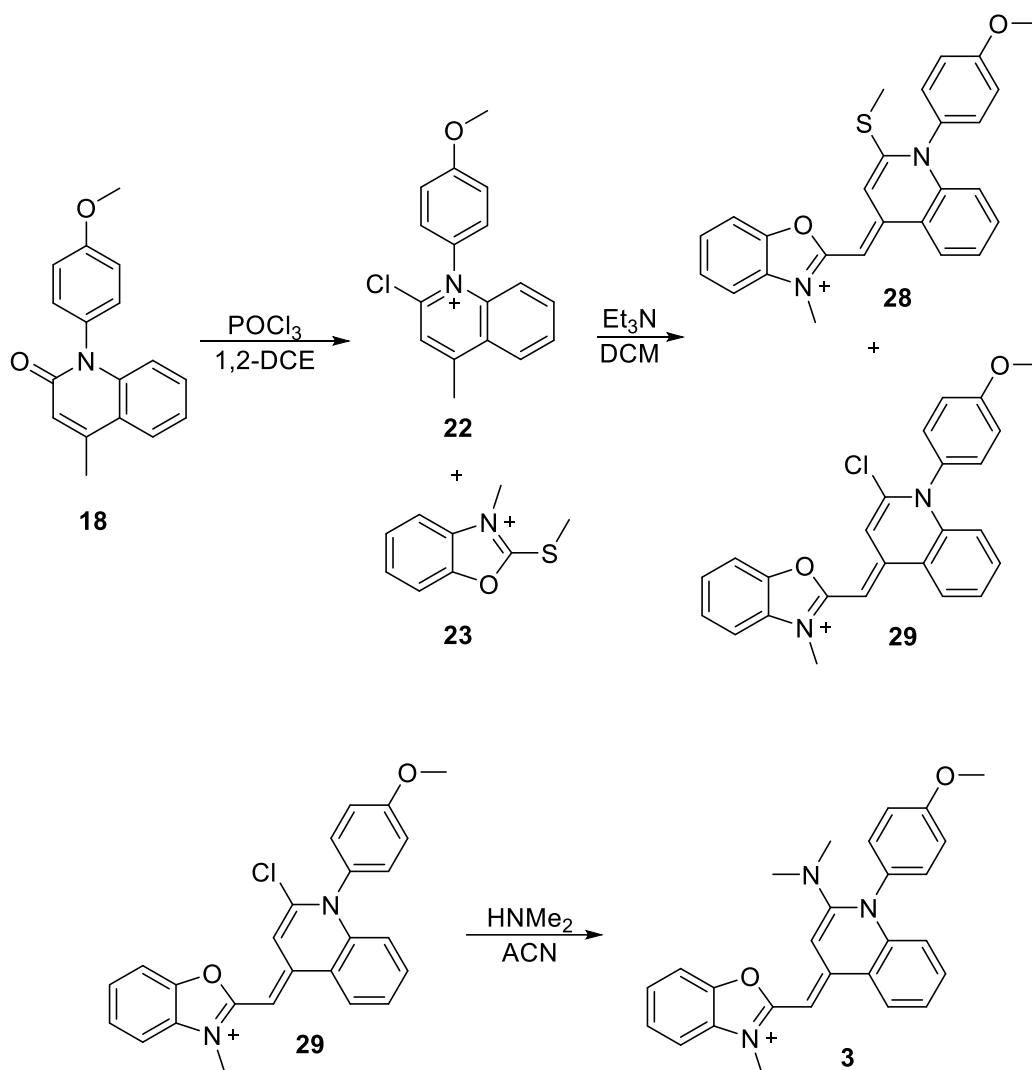


Fig. S8. Synthesis route for dye OxN-OMe 3.

3. NMR Spectra

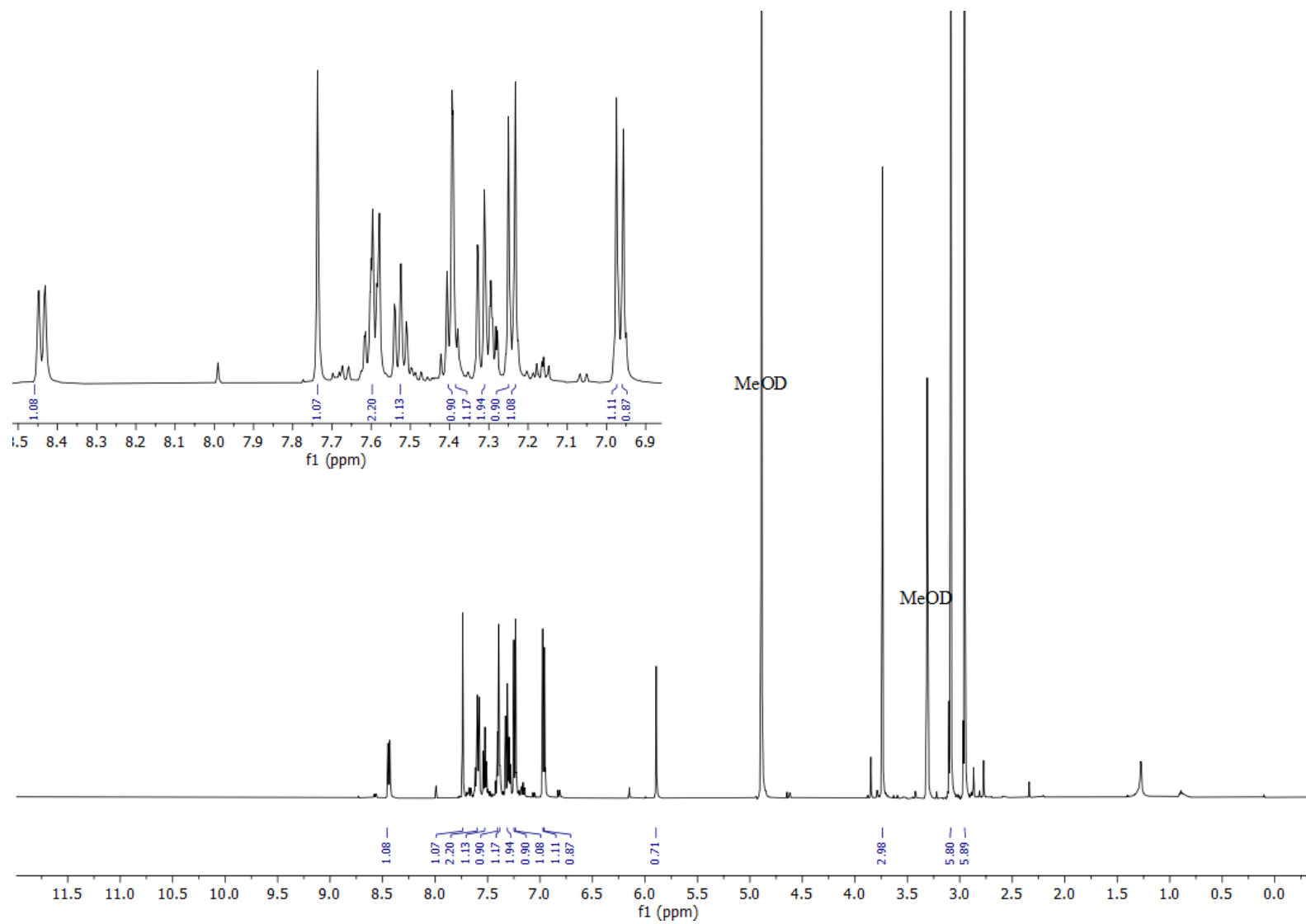


Fig. S9. OxN-NMe₂ (1) ^1H NMR spectra in MeOD.

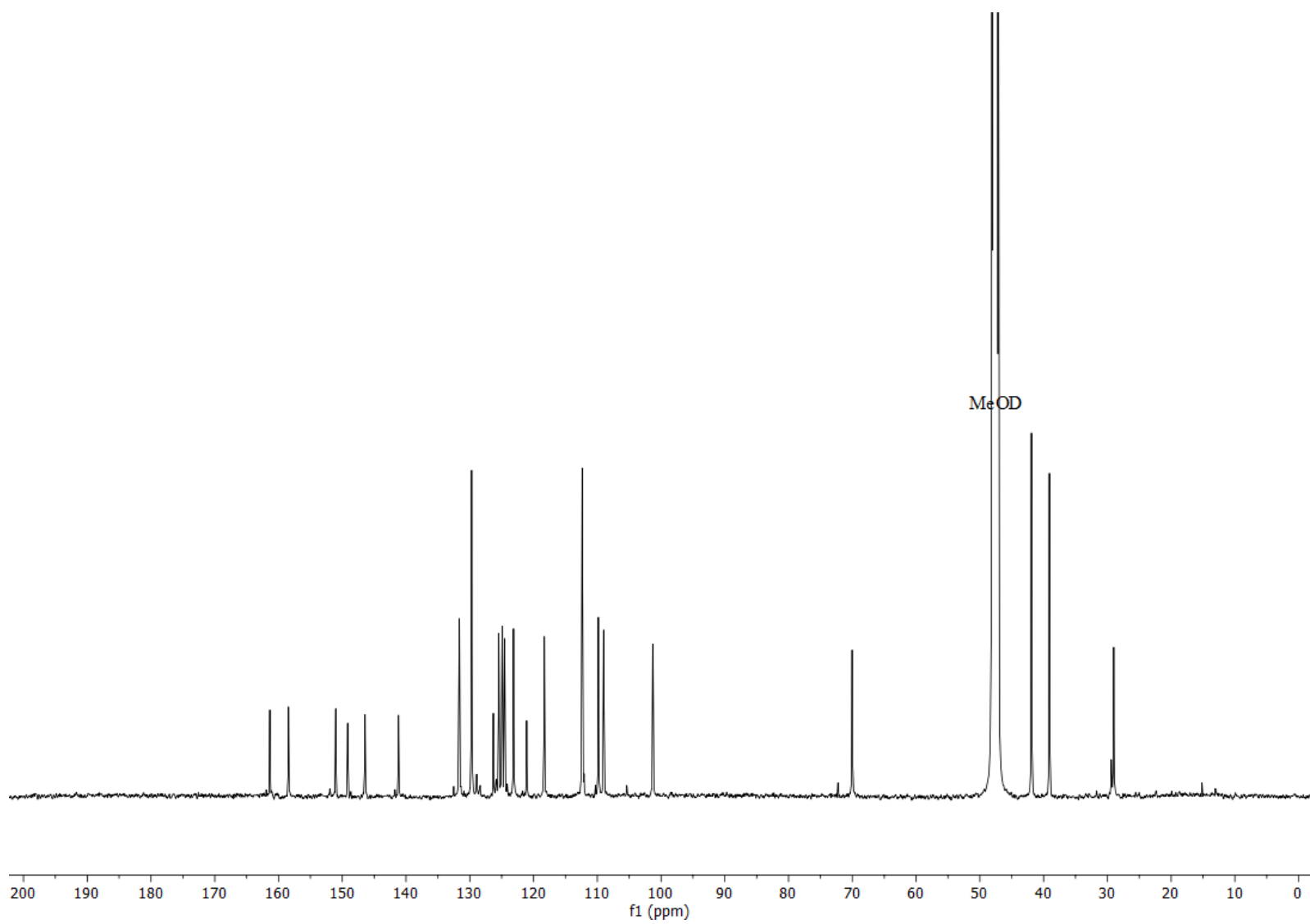


Fig. S10. ^{13}C NMR spectra of OxN-NMe₂ (1) in MeOD.

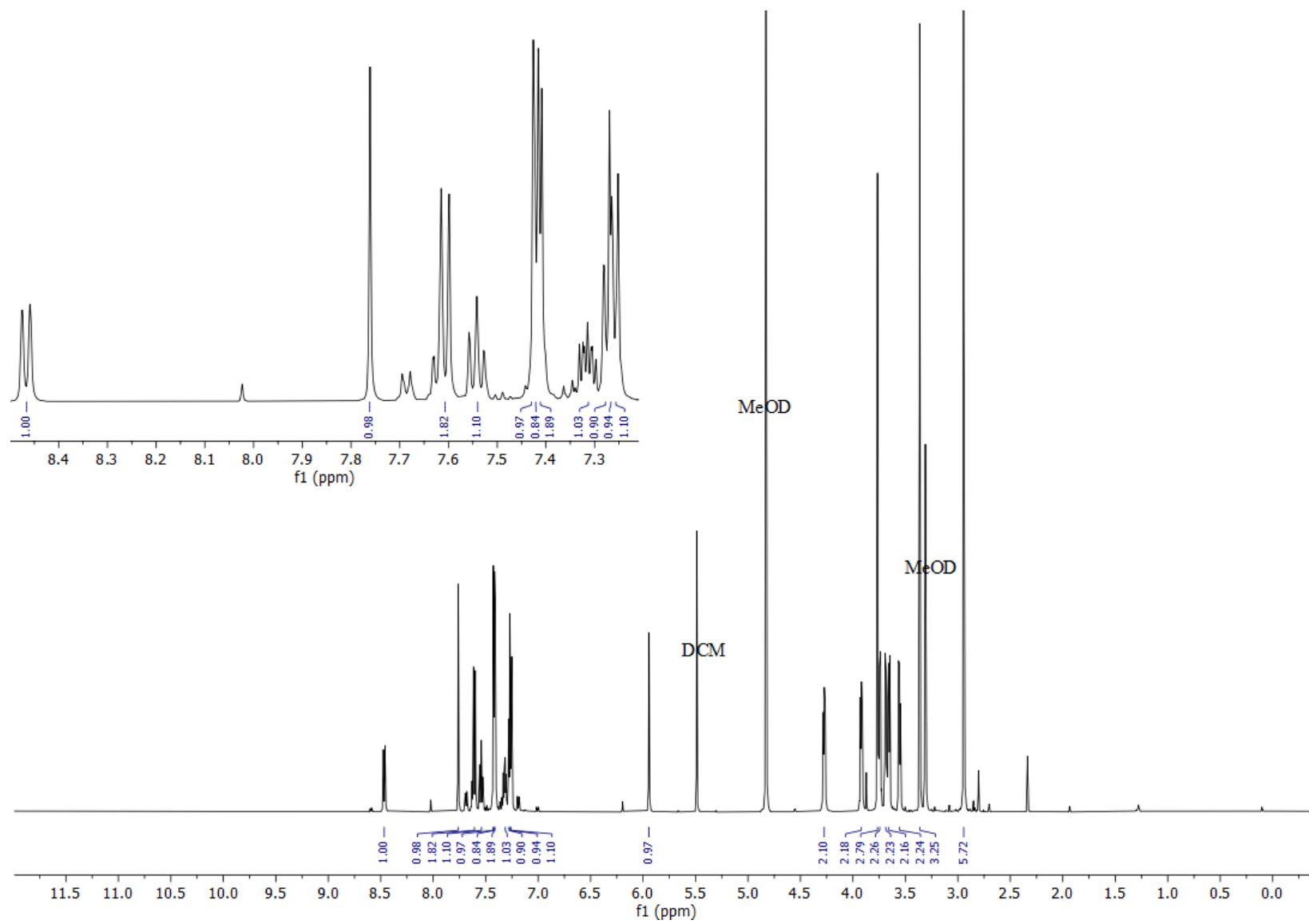


Fig. S11. OxN-PEG (2) ^1H NMR spectra in MeOD.

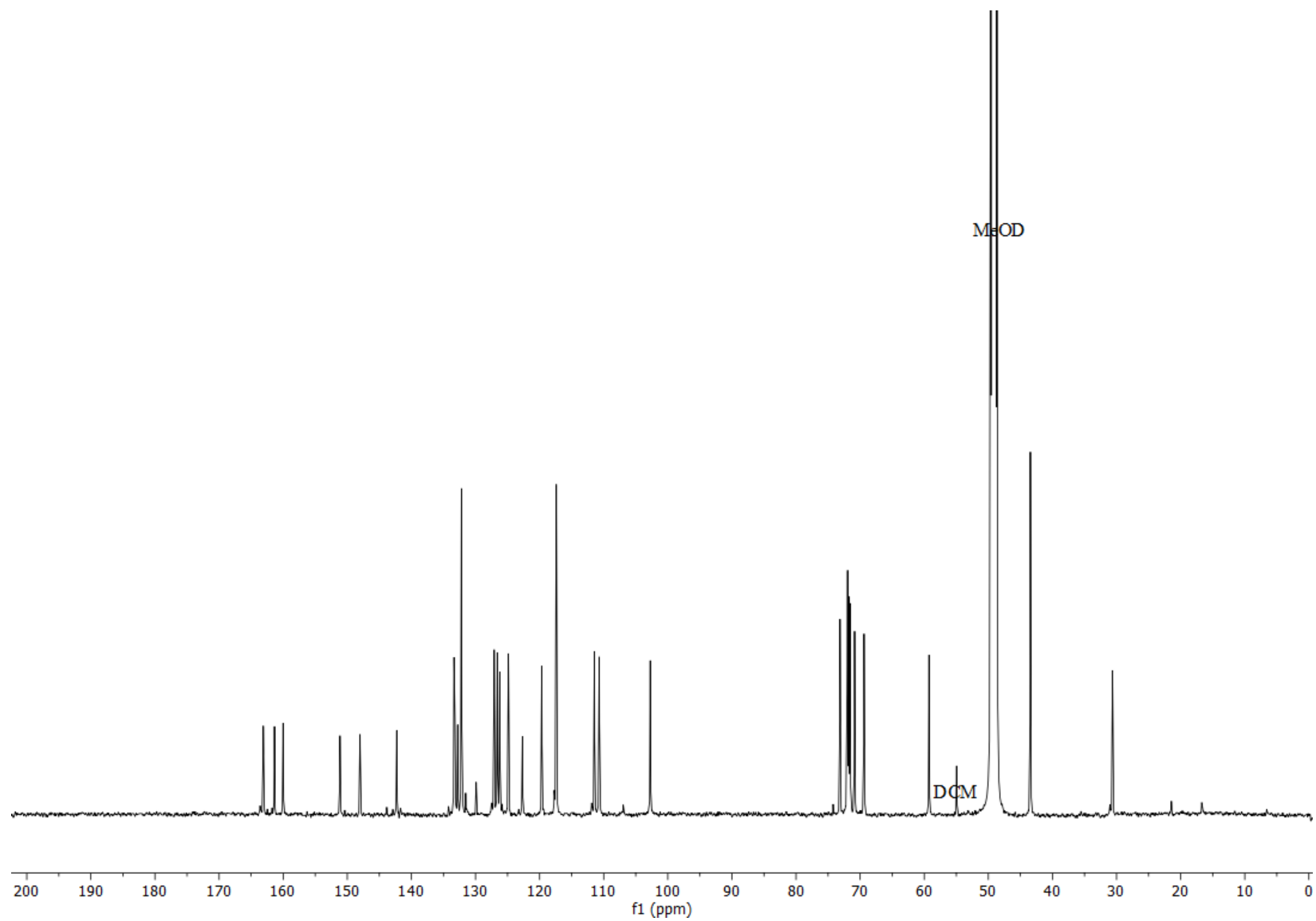


Fig. S12. OxN-PEG (2) ^{13}C NMR spectra in MeOD.

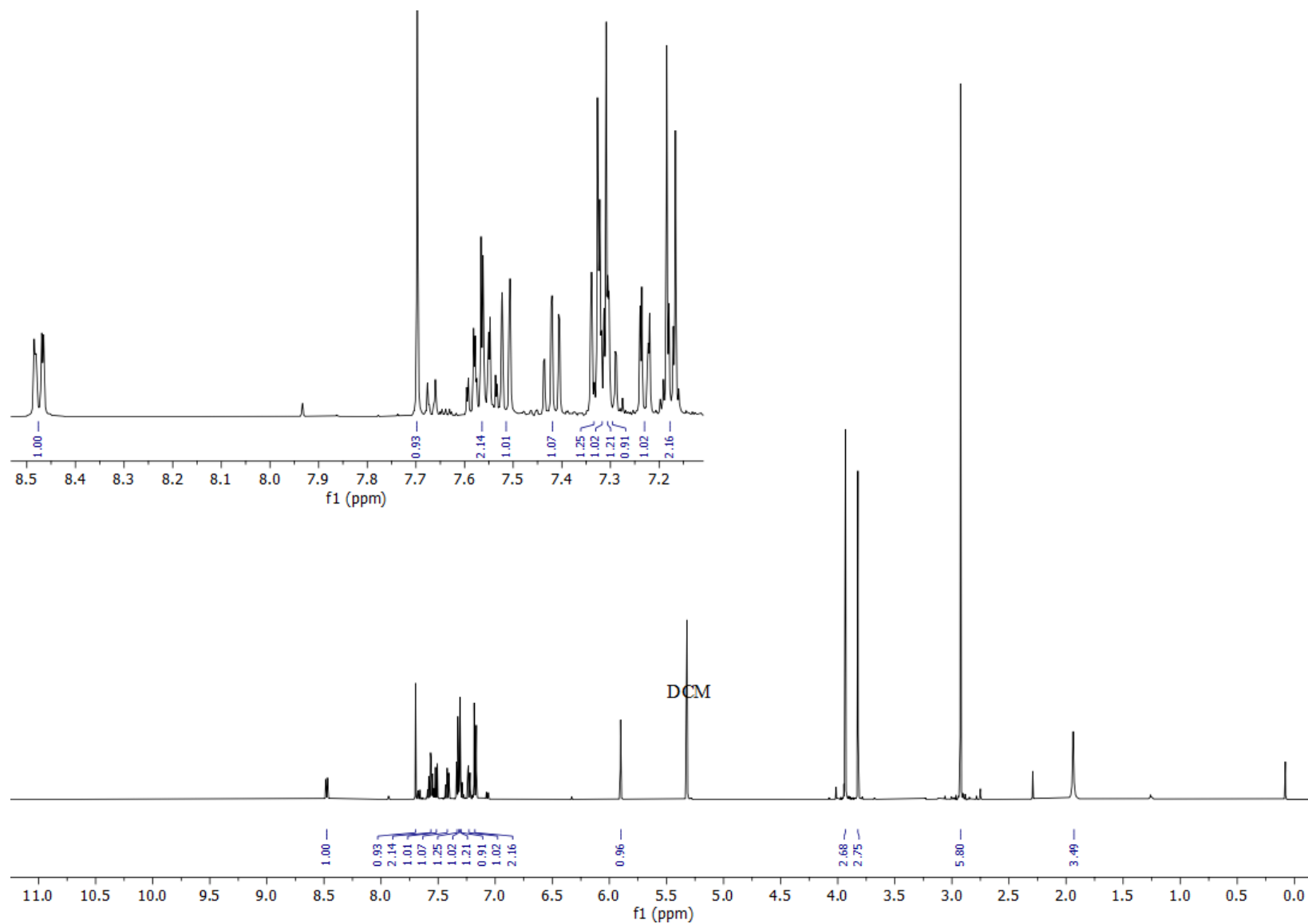


Fig. S13. OxN-OMe (3) ^1H NMR spectra in DCM-d_2 .

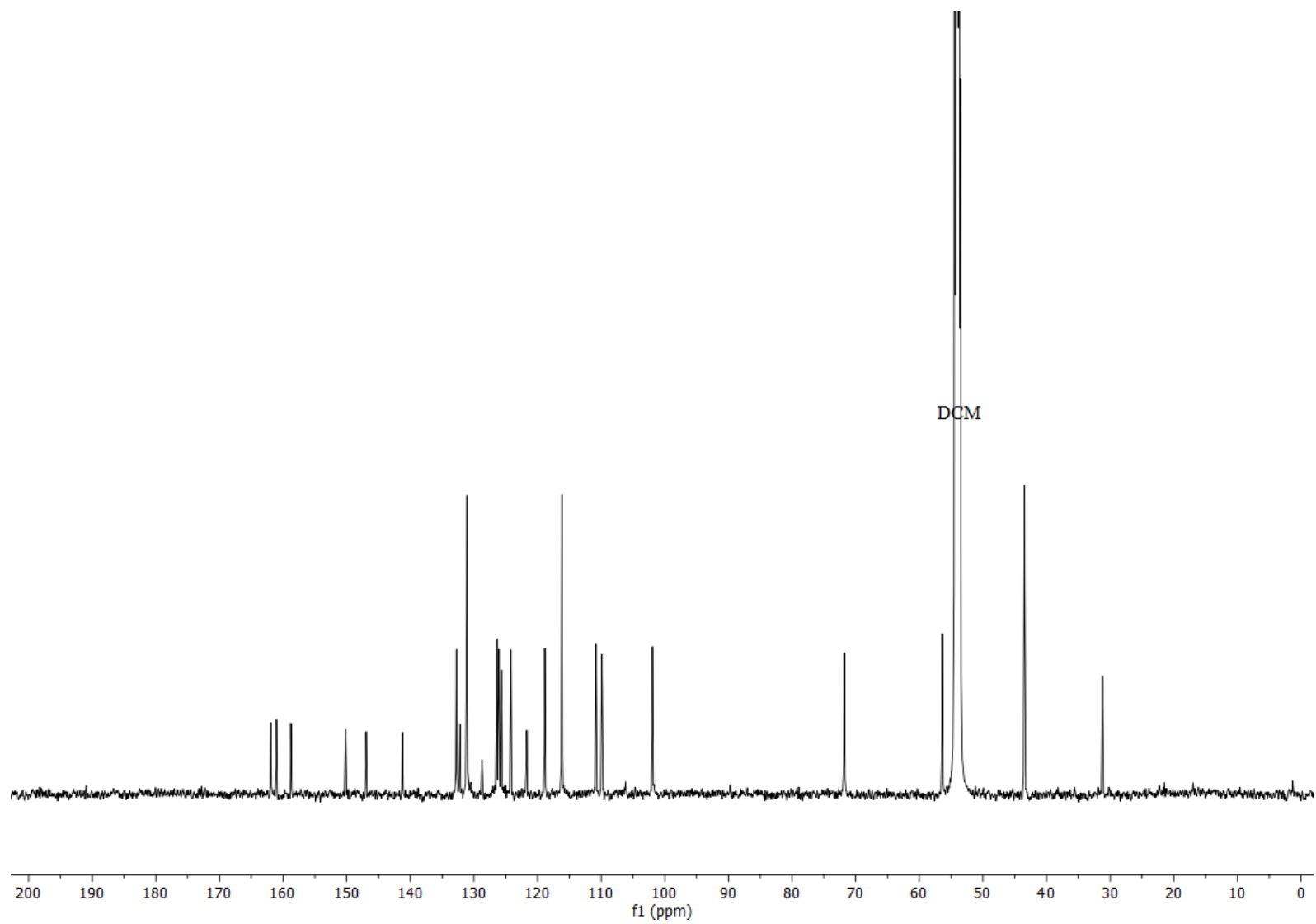


Fig. S14. OxN-OMe (3) ^{13}C NMR spectra in DCM-d_2 .

4. X-ray Diffraction

Suitable single crystals for X-ray diffraction analysis were obtained via slow evaporation of DCM / CH₃CN mixture (1:1 for **1**) or *p*-xylene / CH₃CN (1:1 for **3**) at rt. Single-crystal X-ray data were collected at 120 K by a Rigaku XtaLAB Synergy-R diffractometer equipped with a HyPix-Arc100 detector and an Oxford Cryostream 800 cooling system using mirror-monochromated Cu-K α radiation ($\lambda = 1.54184 \text{ \AA}$). Data collection and reduction for all complexes were performed with the program *CrysAlisPro*⁵ and analytical face-index absorption correction method was applied.⁵ The structure was solved with intrinsic phasing method (*SHELXT*)⁶ and refined by full-matrix least-squares based on F^2 using *SHELXL-2019*.⁷ Anisotropic displacement parameters (ADPs) were introduced for all non-hydrogen atoms. The hydrogen atoms were placed in idealized positions and included as riding, except H atoms of water molecules were found from the electron density maps. Isotropic displacement parameters for all H atoms were constrained to multiples of the equivalent displacement parameters of their parent atoms with $U_{\text{iso}}(\text{H}) = 1.2 U_{\text{eq}}(\text{C})$ or $U_{\text{iso}}(\text{H}) = 1.5 U_{\text{eq}}(\text{O})$. In structure **1**·3H₂O antibumping restraints⁶ (DFIX -1.4, $s = 0.02$) were applied for the H–O–H angles in water molecules to prevent H atoms to end up in too close distances from each other. The O–H distances were also restrained to be more equal (DFIX 0.84, $s = 0.01$). In **3**·0.325CH₃CN·0.5H₂O the bond distances of CH₃CN molecule were made structurally reasonable by hard restraints (DFIX 1.46 and 1.16, $s = 0.001$). The X-ray single crystal data and experimental details as well as CCDC numbers are given below.

Crystal data for 1·2.9H₂O: CCDC-2294210, C_{27.8}H_{34.2}N_{3.9}O_{3.9}Cl_{1.1}, $M = 524.38 \text{ gmol}^{-1}$, orange prisms, $0.10 \times 0.10 \times 0.05 \text{ mm}$, triclinic, space group $P\bar{1}$ (No. 2), $a = 7.76690(10)$, $b = 12.9440(2)$, $c = 14.03810(10) \text{ \AA}$, $\alpha = 79.6140(10)$, $\beta = 83.1530(10)$, $\gamma = 73.8620(10)^\circ$, $V = 1329.92(3) \text{ \AA}^3$, $Z = 2$, $D_{\text{calc}} = 1.309 \text{ gcm}^{-3}$, $F(000) = 556$, $\mu = 1.691 \text{ mm}^{-1}$, $\theta_{\text{max}} = 74.997^\circ$, 106454 reflections, 5470 independent and 5053 with $I > 2\sigma(I)$, $R_{\text{int}} = 0.0316$, 370 parameters, 9 restraints, GooF = 1.041, $R_1 = 0.0412$ and $wR_2 = 0.1145 [I > 2\sigma(I)]$, $R_1 = 0.0438$ and $wR_2 = 0.1163$ (all data), largest diff. peak and hole $0.387 / -0.365 \text{ e\AA}^{-3}$.

Crystal data for 3·0.325CH₃CN·0.5H₂O: CCDC-2294211, C_{55.3}H_{55.95}N_{6.65}O₅Cl_{1.6}I_{0.4}, $M = 1001.19 \text{ gmol}^{-1}$, orange needles, $0.39 \times 0.04 \times 0.03 \text{ mm}$, monoclinic, space group $P2_1/n$ (No. 14), $a = 9.21834(4)$, $b = 21.85441(10)$, $c = 24.63787(9) \text{ \AA}$, $\beta = 94.2872(3)^\circ$, $V = 4949.69(4) \text{ \AA}^3$, $Z = 4$, $D_{\text{calc}} = 1.344 \text{ gcm}^{-3}$, $F(000) = 2091$, $\mu = 3.390 \text{ mm}^{-1}$, $\theta_{\text{max}} = 79.060^\circ$, 201293 reflections, 10470 independent and 10072 with $I > 2\sigma(I)$, $R_{\text{int}} = 0.0415$, 673 parameters, 2 restraints, GooF = 1.090, $R_1 = 0.0567$ and $wR_2 = 0.1417 [I > 2\sigma(I)]$, $R_1 = 0.0582$ and $wR_2 = 0.1426$ (all data), largest diff. peak and hole $0.863 / -0.780 \text{ e\AA}^{-3}$.

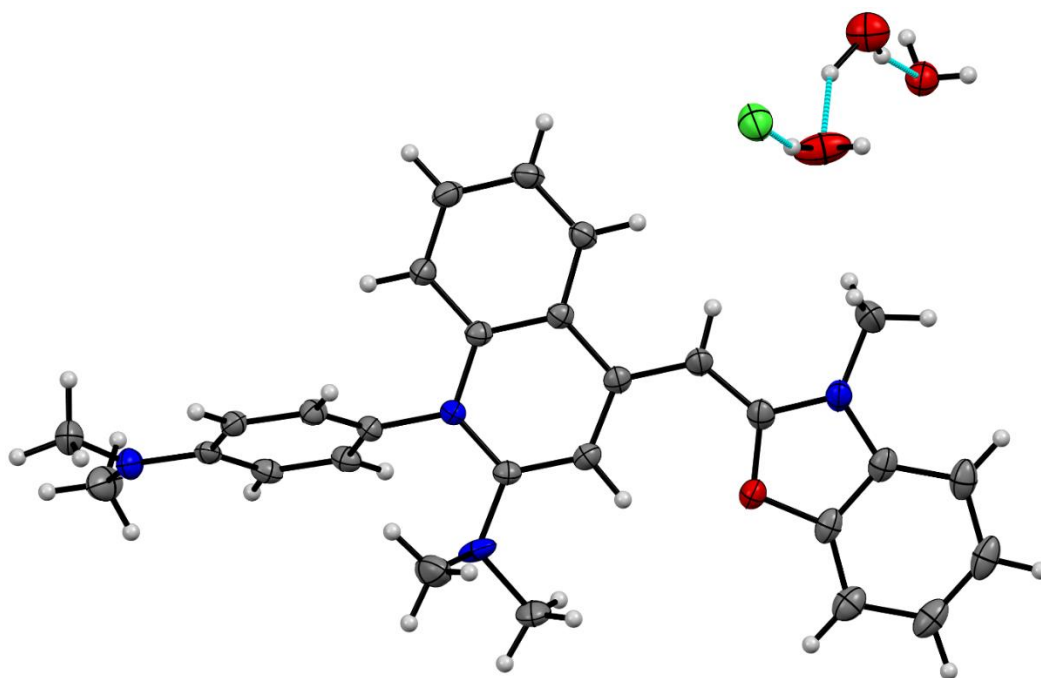


Fig. S15. Crystal structure of **1**·3H₂O (ellipsoid probability 50%). The disorder originated from 10% impurity of compound **25** in the crystal is removed for clarity.

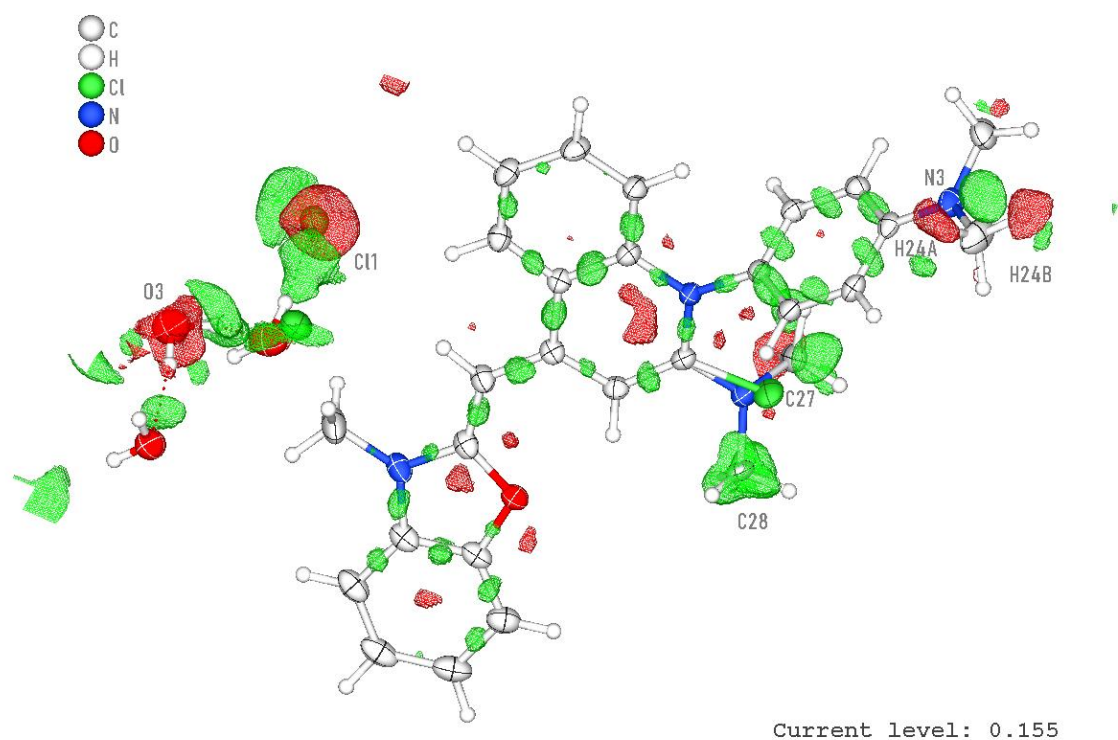


Fig. S16. The residual electron density map around dye **1**. The anomalous residual electron density was treated as positionally disordered chloride anion (90:10) and three water molecules (one of the with 0.9 occupancy). The 10% chloride anion and 90% water molecule occupy nearly the same position of the unit cell. The charge of the mono-cationic **1** is thus - balanced with two chloride anion positions with 90% and 10% occupancy.

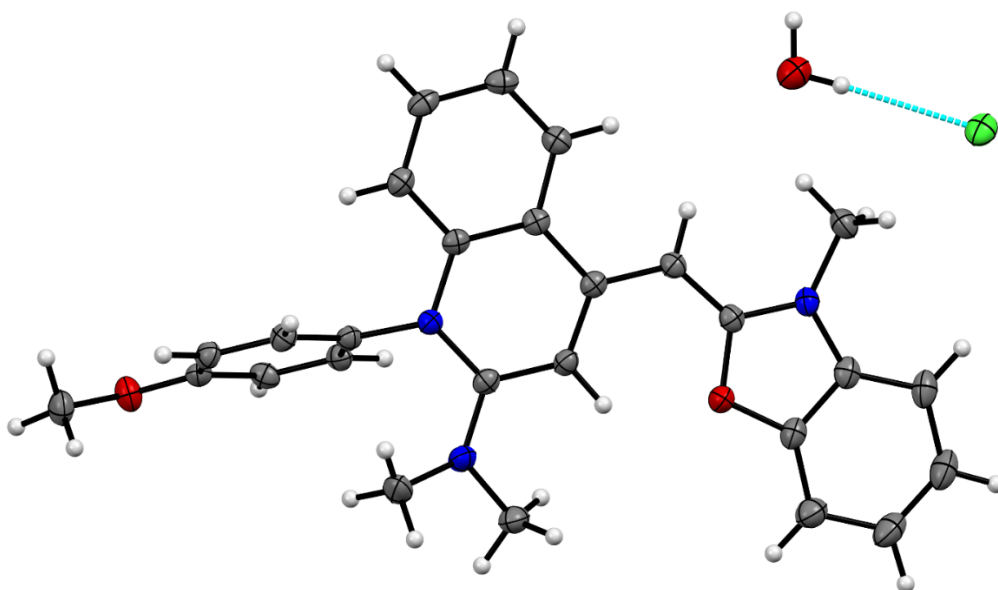


Fig. S17. Crystal structure of **3**·0.325CH₃CN·0.5H₂O (ellipsoid probability 50%), showing one molecule of **3** and water. Another cation and other constituents (0.6 Cl⁻, 0.4 I⁻ and 0.65 CH₃CN) of the asymmetric unit are removed for clarity.

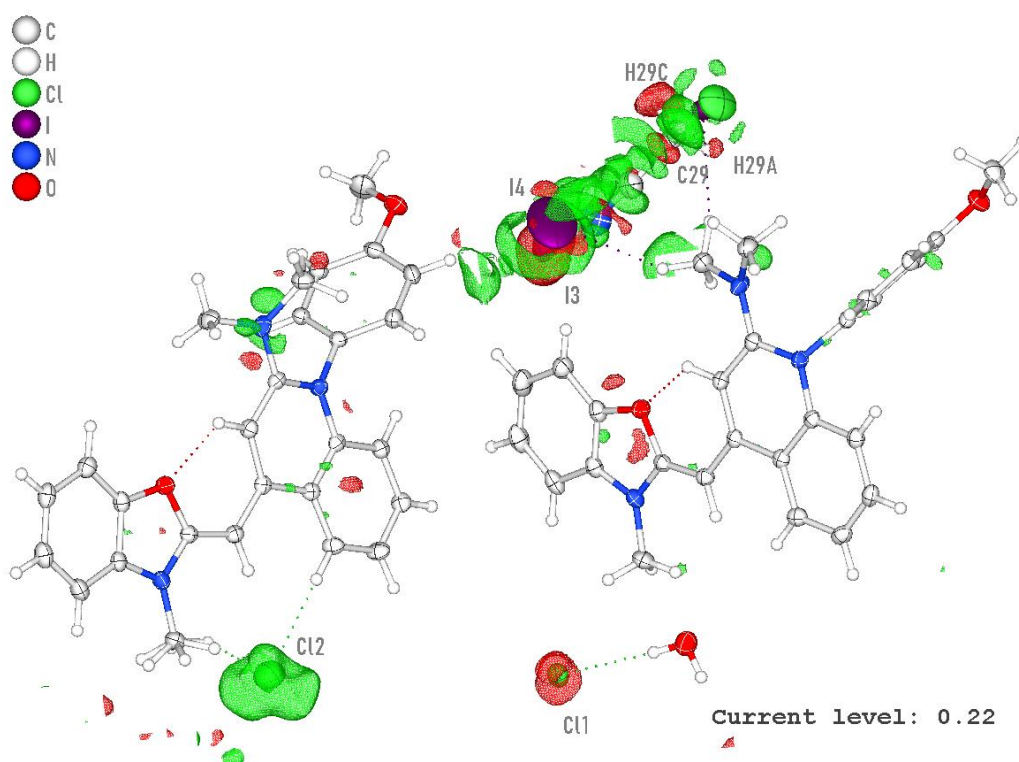


Fig. S18. The residual electron density map around two molecules of dye **3** in the asymmetric unit. The anomalous residual electron density was treated as positionally disordered chloride and iodide anions (1.6:0.4), one water and 0.65 acetonitrile molecules. The residual densities close to the disordered acetonitrile molecule are too high to be chloride anions, and they are thus modelled as disordered iodide anions. The iodide anion results in from one of the

starting compounds. The charge of the two mono-cationic **3** is thus balanced with 1.6 chloride and 0.4 iodide anions.

5. Computational Studies

5.1 General

The geometry calculations for **OxN-NMe₂** (**1**), **OxN-OMe** (**3**) and **PyrON**⁸ were done at the M06-2X/def2-TZVP level of theory⁹ and the SPARTAN20 program¹⁰ with acetonitrile (dielectric = 37.50) as a solvent using conductor like polarizable continuum model (C-PCM).^{11,12} The initial models were built using SPARTAN20 and optimized at MM-level before the DFT calculations. The optimized structures with relevant geometrical parameter are given in Fig. S17.

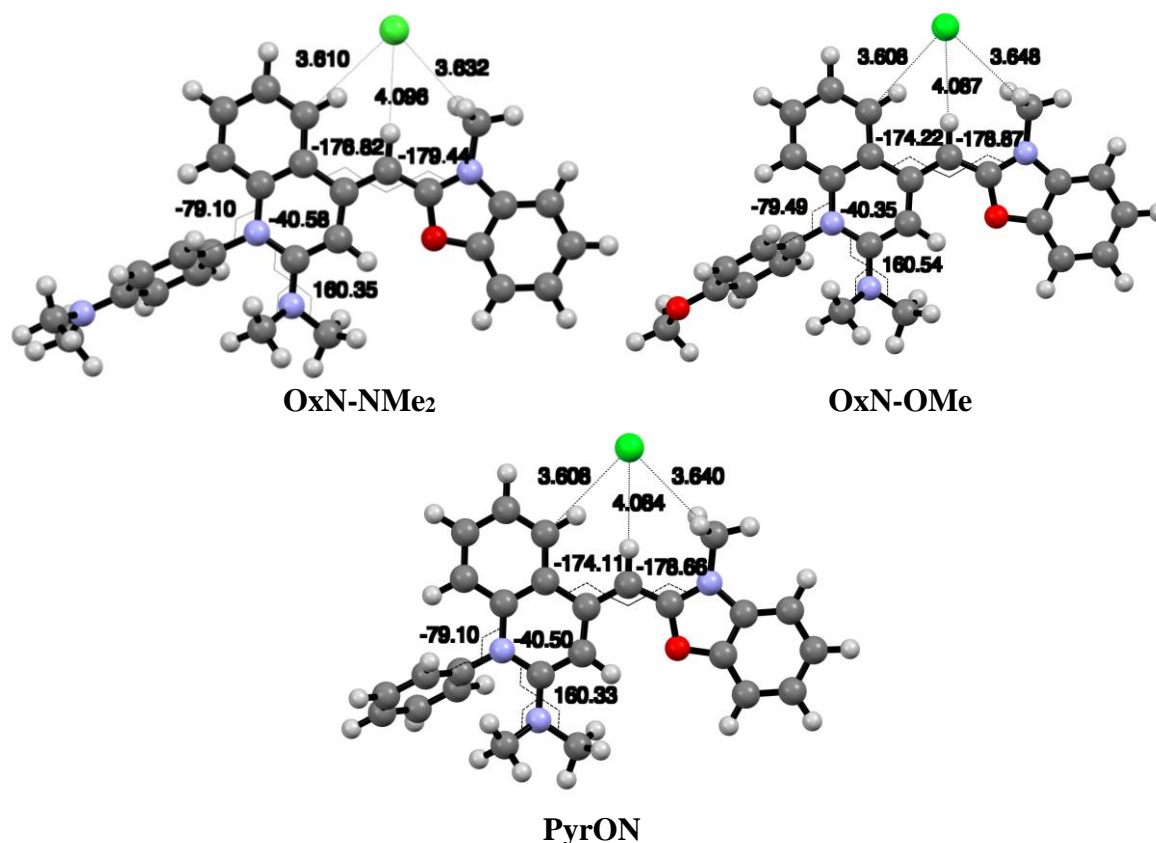


Fig. S19. The DFT optimized structures of **OxN-NMe₂**, **OxN-OMe** and **PyrON**¹² with selected torsion angles H-bond (C...H) distances.

5.2 The Cartesian Coordinates

OxN-NMe₂ (**1**)

H	-0.257203	-1.556257	-1.364577
C	0.023720	-0.602276	-0.960720
C	0.321749	0.451589	-1.809443
N	0.586501	0.631212	1.013590
C	0.800146	1.677604	-1.182282
C	0.165828	-0.528238	0.431056
C	0.918130	1.738284	0.220045
C	1.139723	2.818859	-1.930040
H	1.411261	2.992968	1.905364
C	1.571117	3.974664	-1.324428
H	1.061984	2.812787	-3.008659
H	1.826885	4.835924	-1.927741
C	1.664679	4.028133	0.067235
H	1.990177	4.935732	0.559271
C	1.341135	2.929680	0.830954
C	0.441375	0.823841	2.436895
C	0.113627	1.184010	5.205449
C	1.549496	0.905224	3.265872
C	-0.828951	0.926945	2.979101
C	-0.998719	1.092608	4.341706
C	1.398227	1.083892	4.626414
H	2.542930	0.817957	2.841097
H	-1.695638	0.863145	2.331746
H	-2.002388	1.156516	4.734146
H	2.283339	1.137695	5.242560
N	-0.045063	1.365950	6.549529
N	-0.128884	-1.598632	1.202285
C	1.111344	1.312620	7.421746
H	1.829615	2.095283	7.168938
H	1.624256	0.346986	7.362085
H	0.786799	1.470377	8.446109
C	0.669081	-1.988356	2.364947
H	1.657997	-1.541186	2.318506
H	0.787050	-3.071329	2.329045
H	0.188737	-1.712204	3.305052
C	-1.372511	1.301855	7.127824
H	-1.297890	1.461346	8.199441
H	-1.848377	0.331414	6.951196
H	-2.019369	2.077806	6.713465
C	-0.965038	-2.661698	0.662239
H	-1.412213	-3.189751	1.502452
H	-0.384894	-3.374460	0.067590
H	-1.764084	-2.245658	0.053336
C	0.218705	0.376316	-3.224342
H	0.542819	1.210304	-3.828660
C	-0.268145	-0.680386	-3.954841
O	-0.752785	-1.829628	-3.432243
C	-1.150958	-2.633423	-4.475282
C	-1.771376	-3.820316	-6.838628
C	-0.906614	-1.963786	-5.664563
C	-1.698701	-3.889992	-4.410185
C	-2.009155	-4.480742	-5.634795
C	-1.214254	-2.544506	-6.881312
H	-1.875296	-4.385902	-3.465646
H	-2.442964	-5.471430	-5.646882
H	-1.032998	-2.038158	-7.819417
H	-2.025609	-4.310648	-7.768823
N	-0.351156	-0.743781	-5.305870
C	0.064028	0.319263	-6.199361
H	-0.085516	-0.013818	-7.222591
H	1.115810	0.554400	-6.040317
H	-0.525207	1.216379	-6.014287
Cl	1.383683	3.616994	-5.442348

OxN-OMe (3)

H	-0.184420	-1.524742	-0.795756
C	0.124891	-0.564960	-0.427536
C	0.436270	0.452331	-1.315891
N	0.763292	0.715367	1.492602

C	0.964473	1.682812	-0.739303
C	0.296723	-0.450361	0.956820
C	1.114819	1.785919	0.657138
C	1.315499	2.789988	-1.530642
H	1.685257	3.080290	2.288769
C	1.793215	3.951980	-0.972856
H	1.206105	2.752562	-2.605596
H	2.055116	4.787399	-1.609096
C	1.924445	4.045743	0.413187
H	2.288766	4.958072	0.867667
C	1.587302	2.982264	1.219285
C	0.627083	0.969085	2.907459
C	0.314889	1.458543	5.618400
C	1.746739	1.050752	3.727342
C	-0.637818	1.140177	3.434642
C	-0.804897	1.378452	4.794468
C	1.593775	1.298282	5.074716
H	2.733877	0.913908	3.302677
H	-1.503439	1.079489	2.786260
H	-1.802315	1.502086	5.189937
H	2.452594	1.365162	5.729728
N	-0.009757	-1.485327	1.769705
C	0.799872	-1.853634	2.931001
H	1.792651	-1.418587	2.858456
H	0.906029	-2.937951	2.923103
H	0.335628	-1.547639	3.869859
C	-0.883834	-2.544490	1.283999
H	-1.323634	-3.033724	2.151204
H	-0.335833	-3.290649	0.700722
H	-1.685123	-2.126615	0.679004
C	0.304590	0.331501	-2.724209
H	0.679983	1.114295	-3.366201
C	-0.274507	-0.714489	-3.402344
O	-0.853163	-1.789889	-2.822060
C	-1.329422	-2.605091	-3.823333
C	-2.072076	-3.844493	-6.124515
C	-1.038103	-2.017179	-5.044427
C	-1.985318	-3.804103	-3.695528
C	-2.357062	-4.422908	-4.889186
C	-1.404497	-2.626338	-6.230707
H	-2.196669	-4.236892	-2.727378
H	-2.877334	-5.370513	-4.851421
H	-1.186530	-2.183850	-7.192920
H	-2.376219	-4.354424	-7.029126
N	-0.377904	-0.833015	-4.747651
C	0.150428	0.127419	-5.695898
H	-0.120913	-0.194247	-6.697132
H	1.235743	0.180691	-5.609173
H	-0.264342	1.115677	-5.502526
Cl	1.404775	3.494179	-5.068147
O	0.262129	1.688683	6.948241
C	-1.016320	1.861215	7.541768
H	-1.531484	2.721367	7.109917
H	-0.836210	2.034483	8.598626
H	-1.627809	0.965939	7.413852

PyrON

H	-0.281295	-1.384176	-0.230619
C	0.028156	-0.424125	0.137296
C	0.340606	0.593324	-0.751279
N	0.677999	0.852528	2.055487
C	0.870468	1.823100	-0.174771
C	0.204284	-0.310730	1.520334
C	1.027789	1.924838	1.221158
C	1.217409	2.930917	-0.966776
H	1.608495	3.218302	2.850645
C	1.701459	4.091047	-0.410580
H	1.099367	2.895872	-2.040990

H	1.962016	4.926362	-1.047490
C	1.839731	4.183400	0.974764
H	2.208038	5.094556	1.428368
C	1.504167	3.120115	1.781928
C	0.540422	1.105620	3.471875
C	0.229597	1.593489	6.172166
C	1.661834	1.196223	4.281520
C	-0.734263	1.265596	3.990652
C	-0.886690	1.503977	5.350489
C	1.504266	1.445375	5.636506
H	2.645914	1.064876	3.848342
H	-1.593757	1.195573	3.335212
H	-1.878535	1.623161	5.766196
H	2.376428	1.516295	6.273231
N	-0.100129	-1.345291	2.334692
C	0.717111	-1.720639	3.488196
H	1.707042	-1.279661	3.414729
H	0.828804	-2.804313	3.469741
H	0.255226	-1.426568	4.432031
C	-0.985044	-2.398157	1.855271
H	-1.422041	-2.884526	2.725572
H	-0.446127	-3.147872	1.268169
H	-1.787484	-1.974351	1.255974
C	0.218670	0.468764	-2.159370
H	0.609790	1.243912	-2.801416
C	-0.363273	-0.576220	-2.837596
O	-0.958671	-1.642037	-2.257002
C	-1.427322	-2.461418	-3.258566
C	-2.158507	-3.706404	-5.560472
C	-1.124054	-1.879868	-4.479759
C	-2.085907	-3.659072	-3.131044
C	-2.451194	-4.280929	-4.325043
C	-1.486981	-2.490503	-5.666406
H	-2.303008	-4.089086	-2.162943
H	-2.972332	-5.228076	-4.287625
H	-1.261772	-2.051684	-6.628624
H	-2.458823	-4.218232	-6.465290
N	-0.454186	-0.701144	-4.182800
C	0.060655	0.267433	-5.130241
H	-0.202348	-0.059404	-6.132005
H	1.144388	0.338369	-5.039421
H	-0.370867	1.249078	-4.938970
Cl	1.299755	3.631623	-4.504796
H	0.104724	1.780761	7.231351

6. UV-vis Spectra

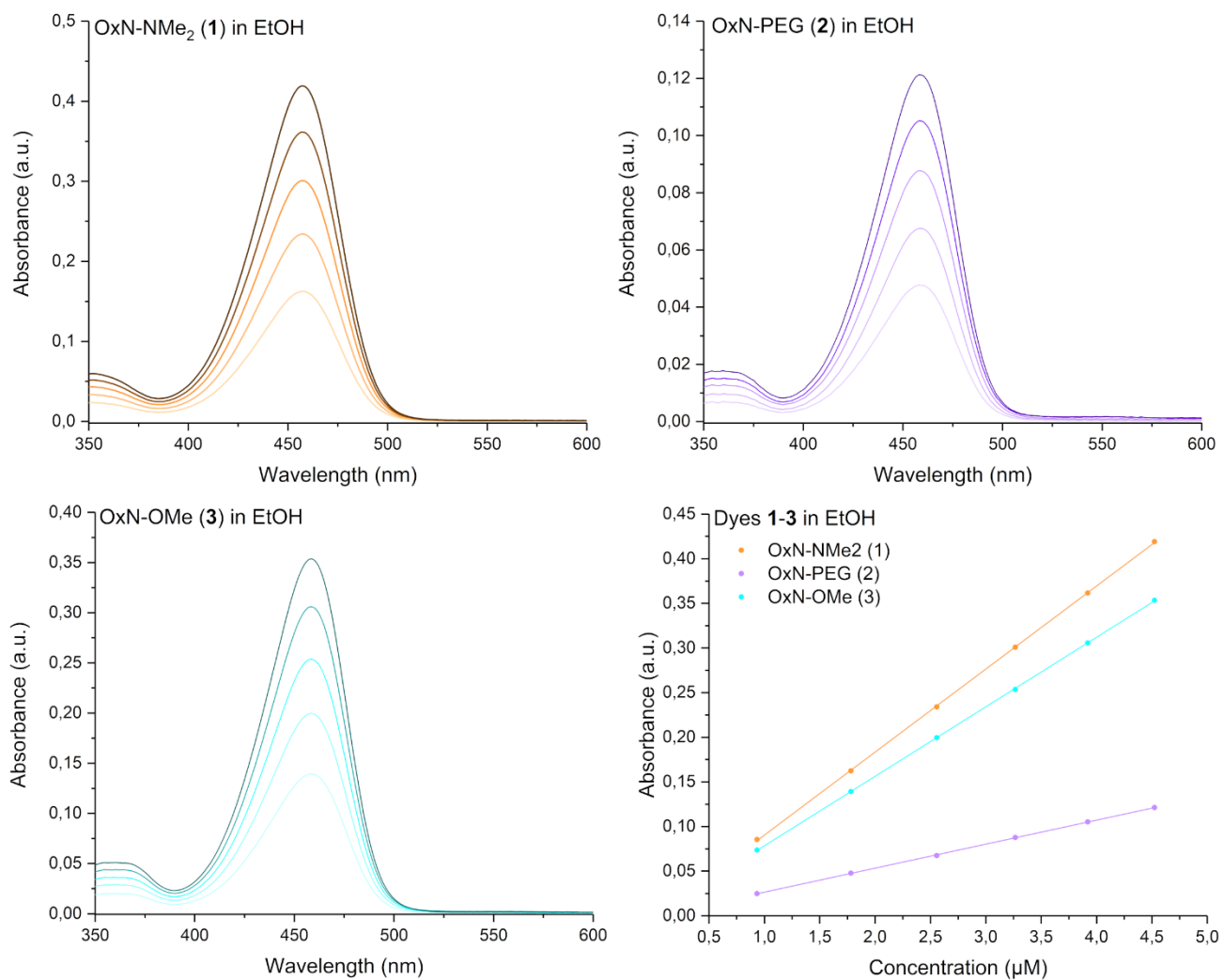


Fig. S20. Absorbance of dyes 1-3 in EtOH in varying dye concentrations.

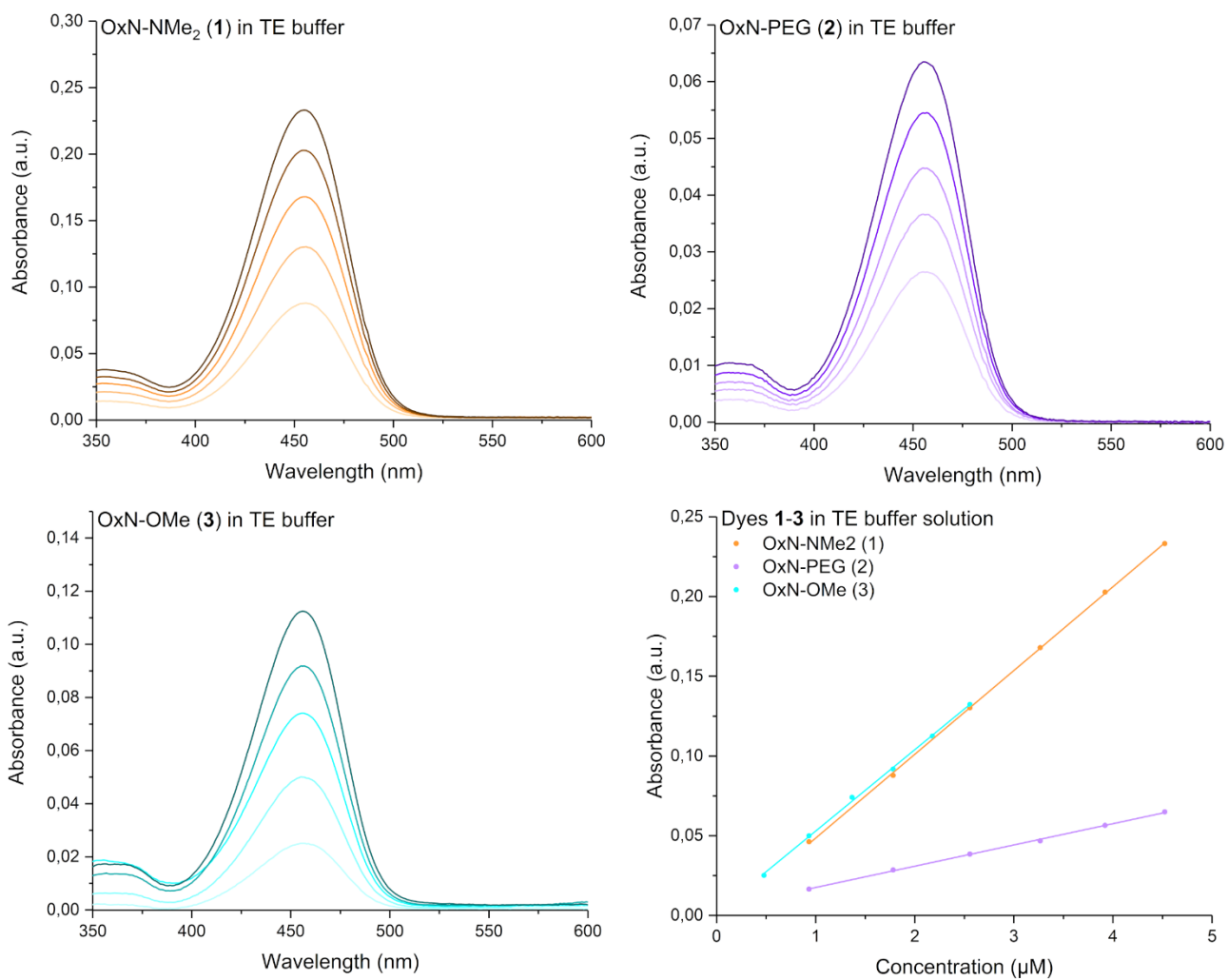


Fig. S21. Absorbance of dyes 1-3 in TE buffer in varying dye concentrations.

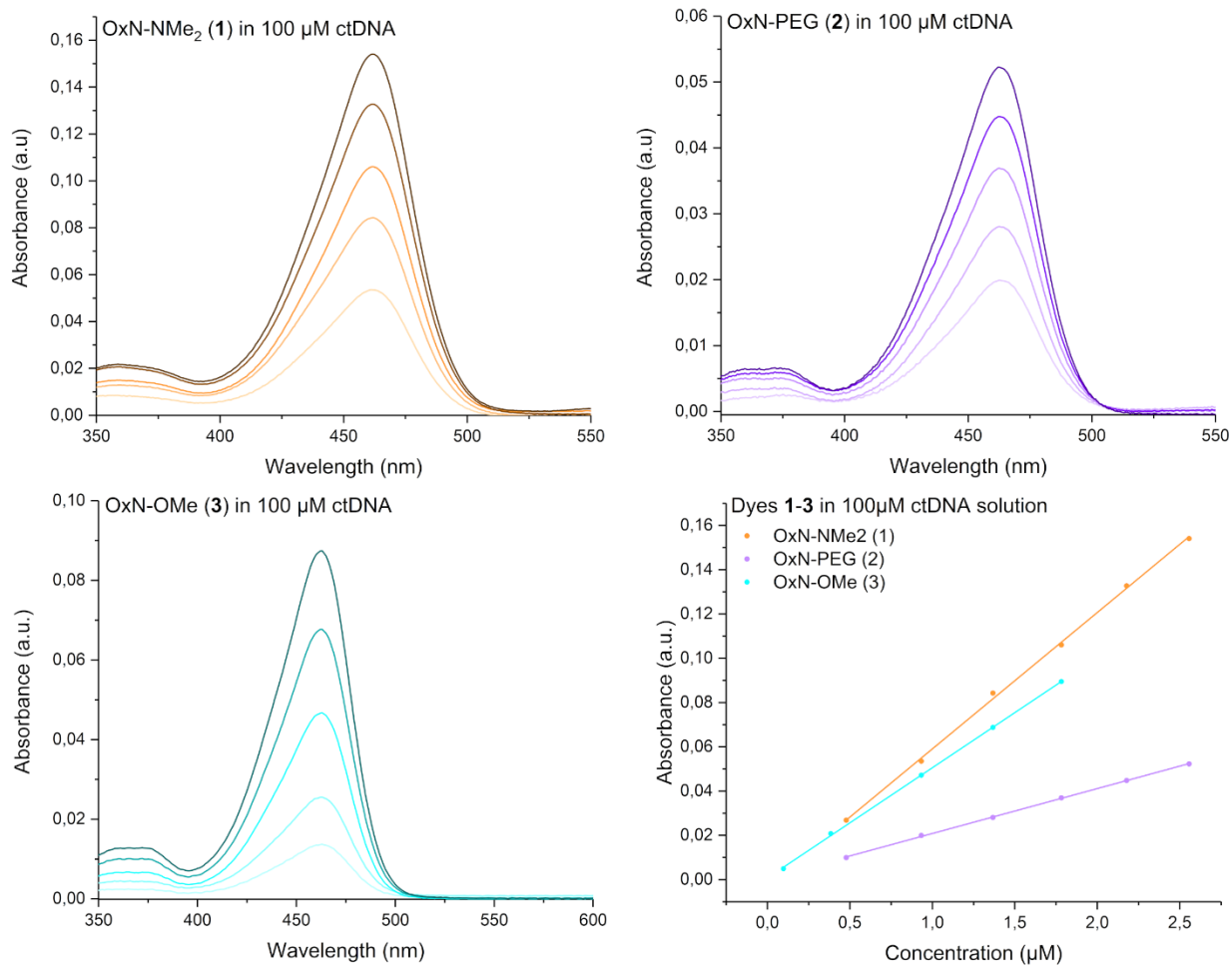


Fig. S22. Absorbance of dyes 1-3 in 100 μM ctDNA solution in varying dye concentrations.

7. Fluorescence Spectra

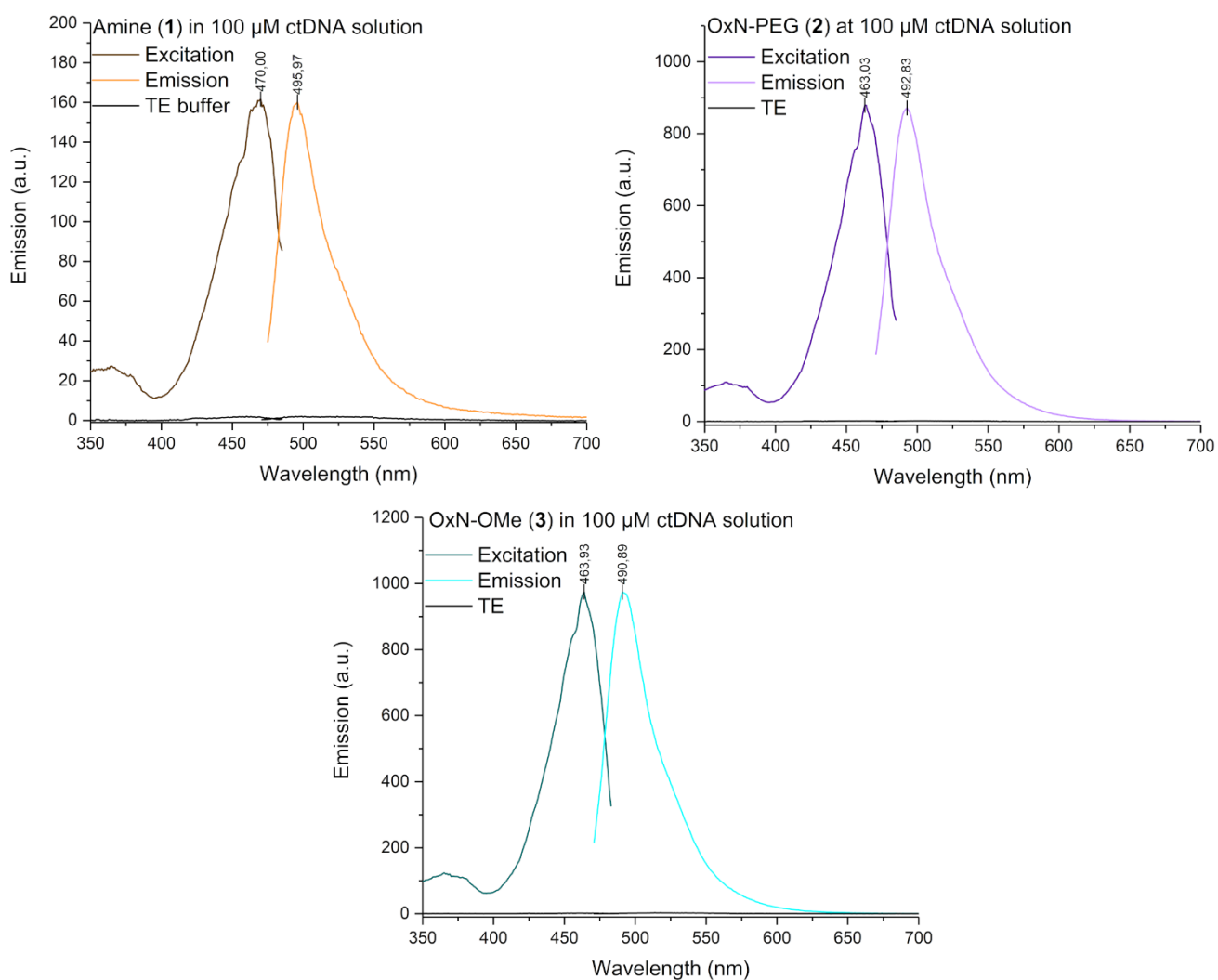


Fig. S23. Emission and excitation of dyes **1-3** in 100 μM ctDNA solution and free dye in TE buffer. Dyes were registered and excited at the unique maxima marked for each dye in their respective plots.

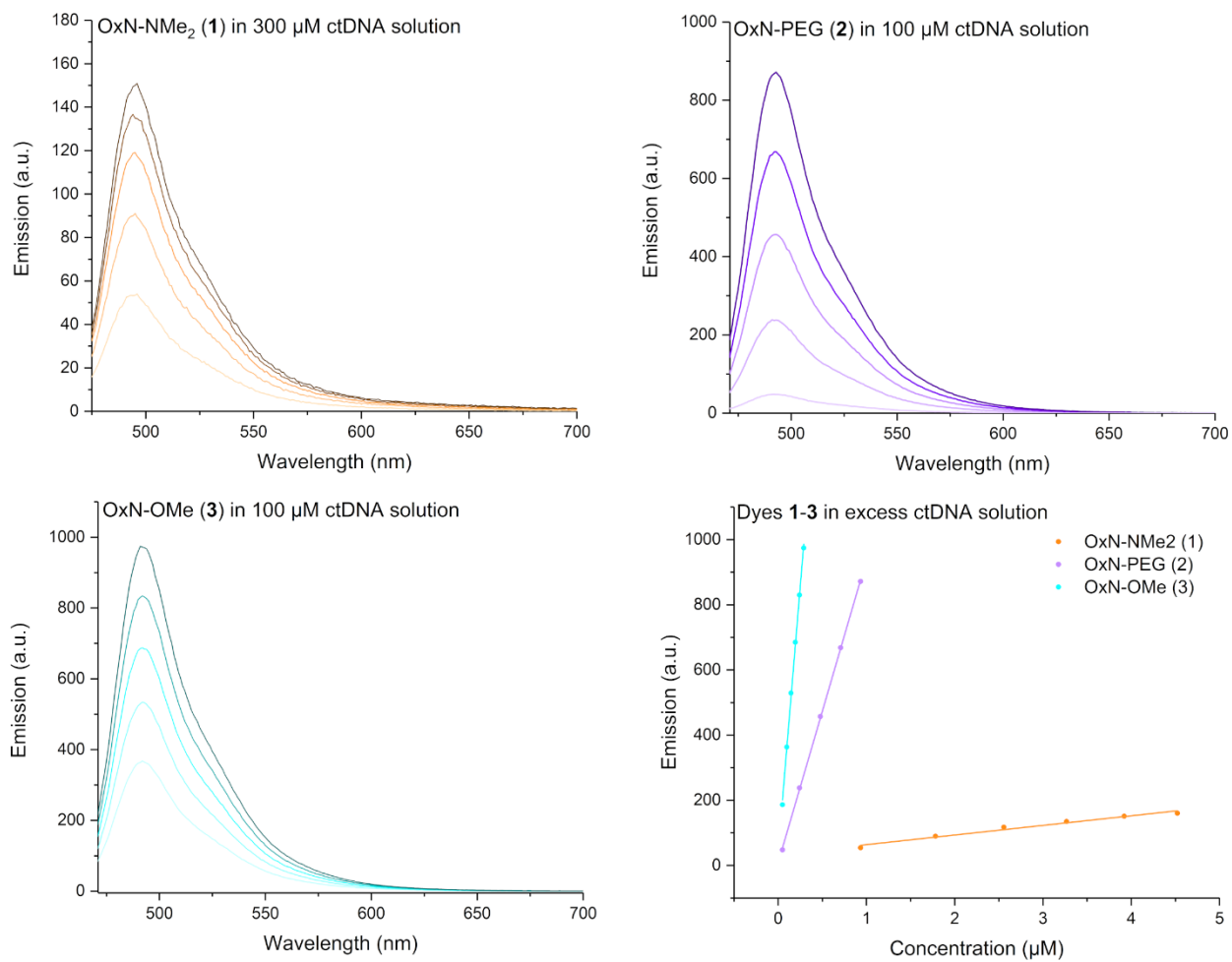


Fig. S24. Emission of dyes 1-3 in excess ctDNA solution in varying dye concentrations and emission maximas plotted against dye concentrations.

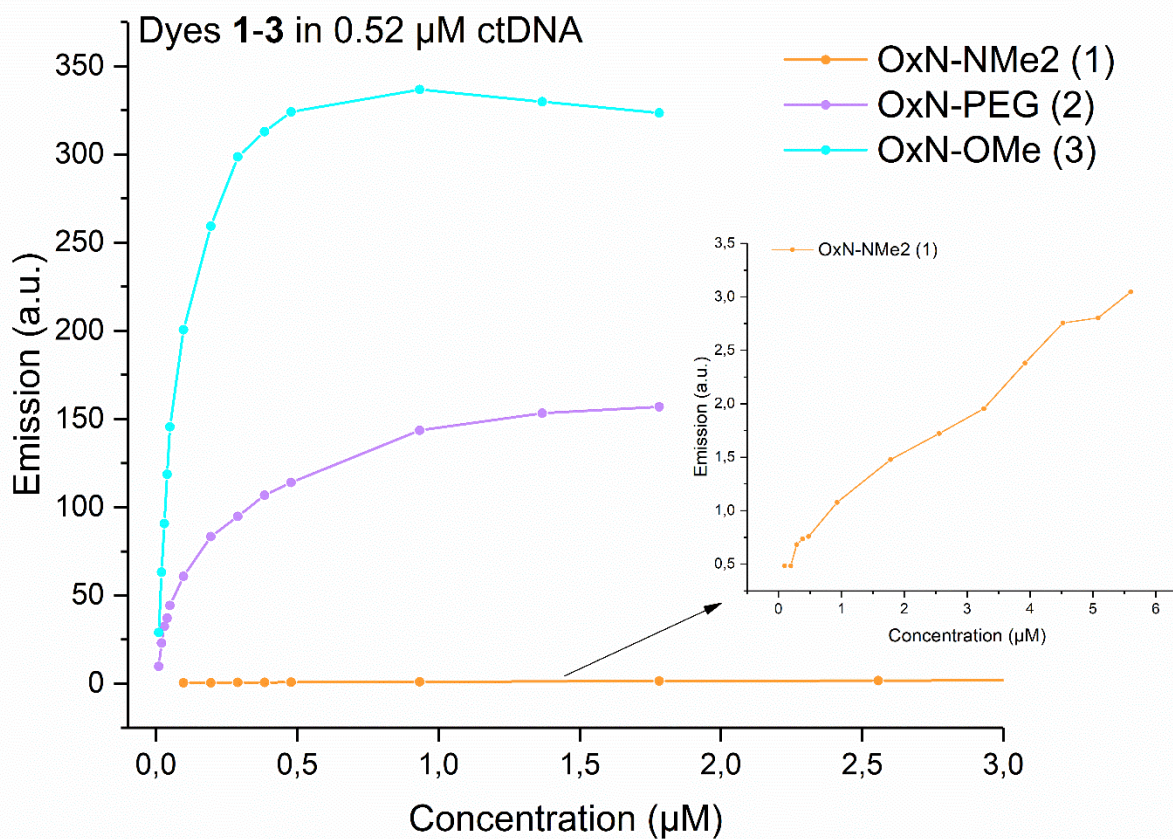


Fig. S25. Titration experiment of dyes **1-3** in 0.52 μM ctDNA solution. OxN-NMe₂ (**1**) was excited at 470 nm, OxN-PEG (**2**) at 463 nm and OxN-OMe (**3**) at 464 nm, respectively.

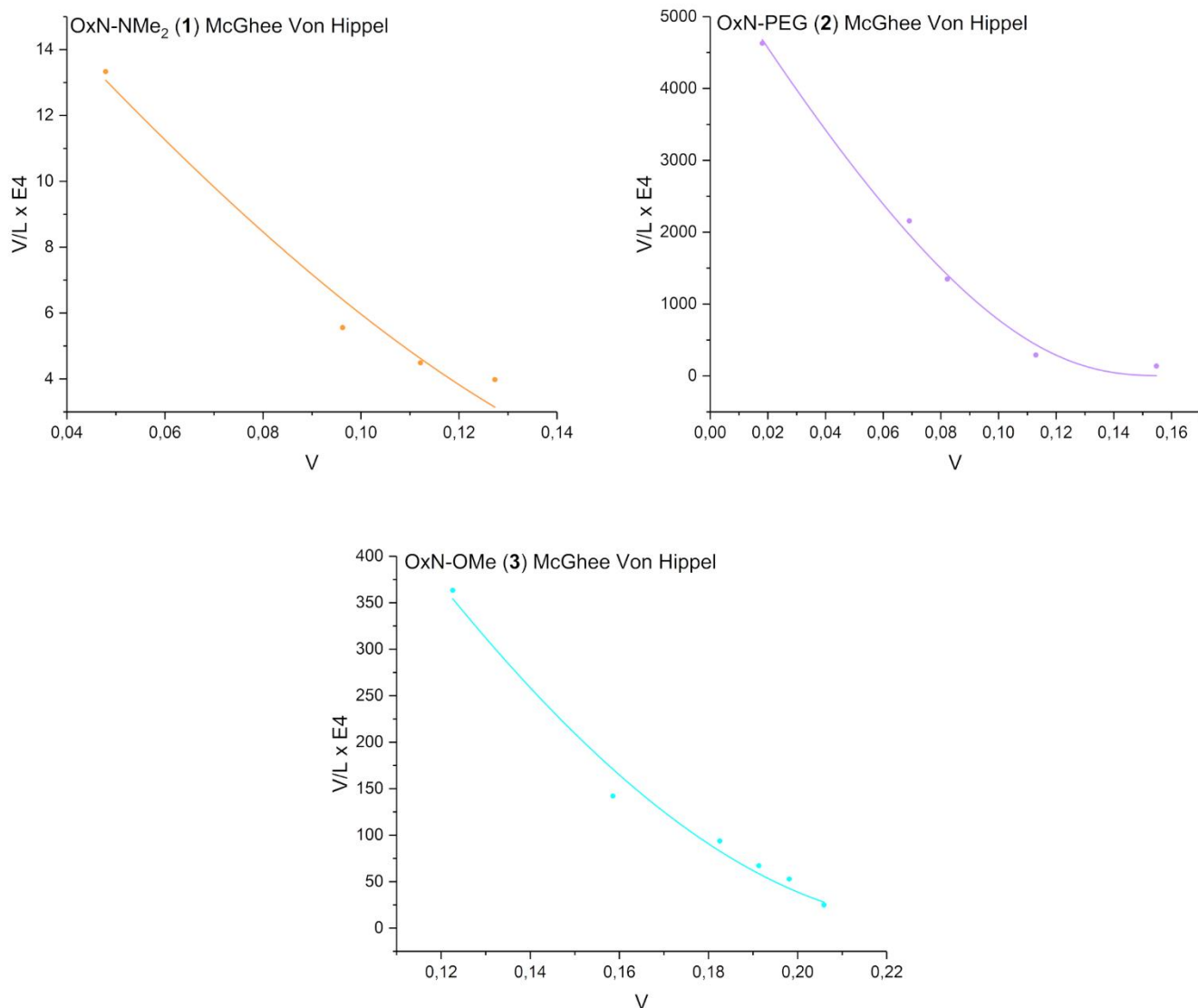
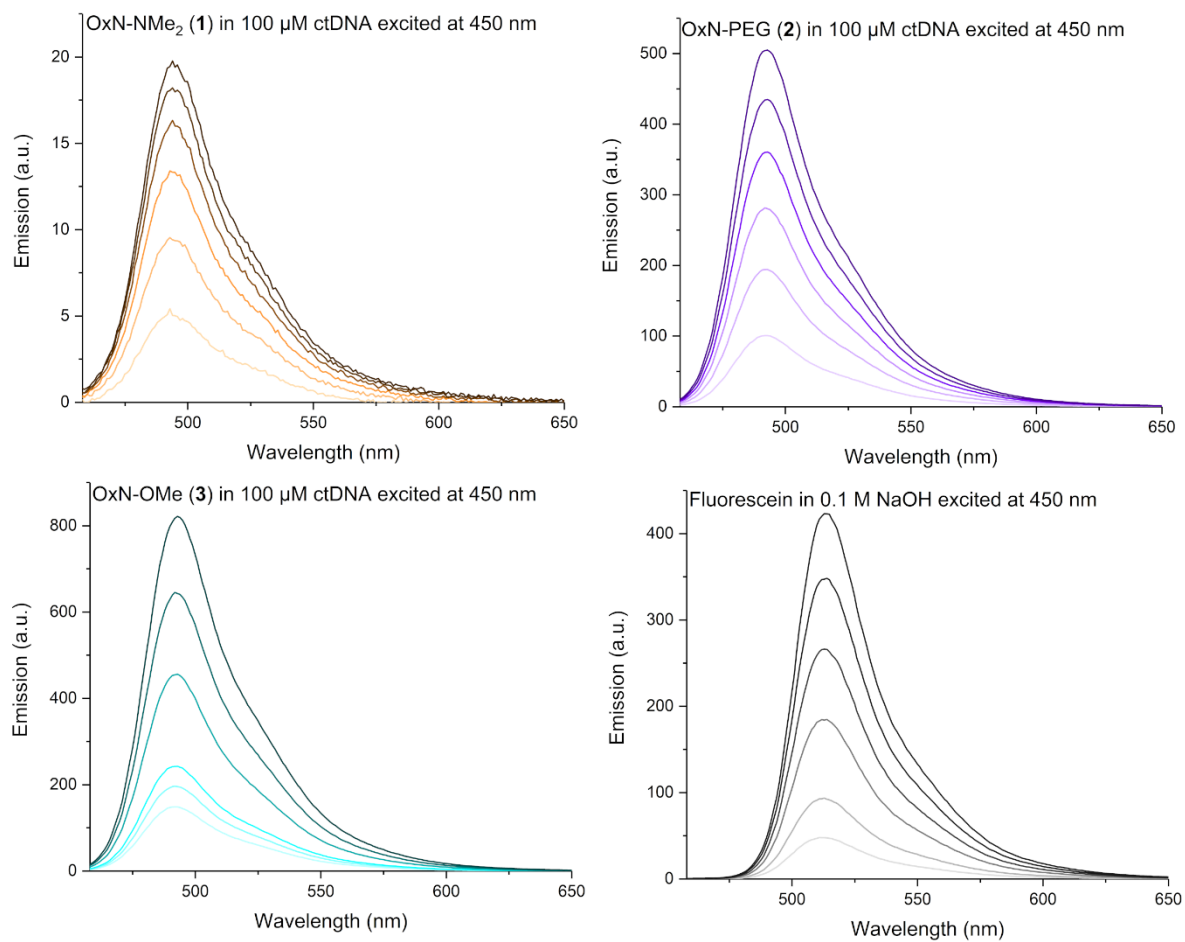


Fig. S26. Processing of data from Fig. S21 and Fig. S23 gave Scatchard plots presenting the ratio of bound and free dye (V/L) as a function of dye molecules bound with the ctDNA (V). Presented lines are the results from fitting McGhee Von Hippel equation of non-cooperative DNA binding.¹³



Fig, S27. Fluorescence titrations of dyes **1-3** and fluorescein for quantum yield measurements. All samples were excited at 450 nm.

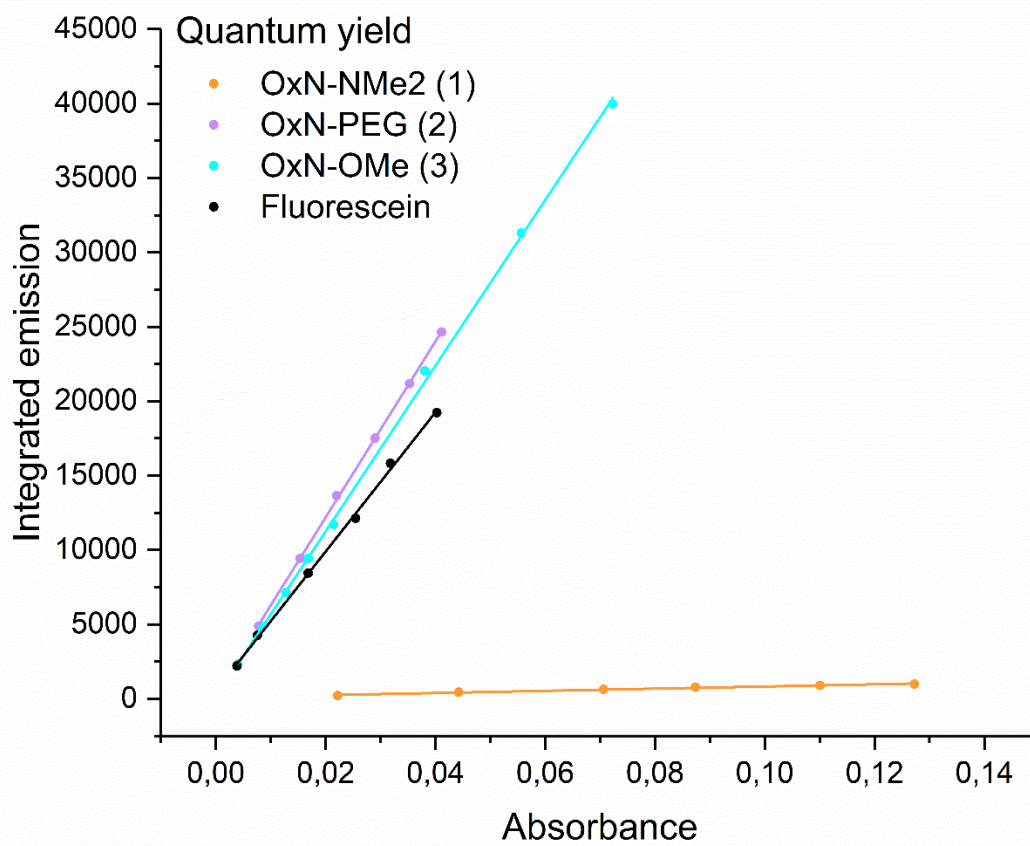


Fig. S28. Quantum yield determination for dyes **1-3** derived from plots **Fig. S20.** and **Fig. S25.** Dyes **1-3** were measured in 100 μ M ctDNA solution and fluorescein standard in 0.1 M NaOH solution. All samples were excited at 450 nm. Measured emission (**Fig. S25.**) was integrated and plotted against absorbance (**Fig. S20.**) at 450 nm for each dye, respectively. These slopes were then used to calculate quantum yields based on the known quantum yield of fluorescein.

8. Literature

1. V. K. Saarnio, K. Salorinne, V. P. Ruokolainen, J. R. Nilsson, T. R. Tero, S. Oikarinen, L. M. Wilhelmsson, T. M. Lahtinen and V. S. Marjomäki, *Dyes and Pigments*, 2020, **177**.

2. *Invitrogen. SYBR® green I nucleic acid gel stain product information sheet, vols. 1–5*, 2006.
3. L. Ying, US Pat., 2013, US20130137875A1.
4. R. Nguyen, N. Jouault, S. Zanirati, M. Rawiso, L. Allouche, G. Fuks, E. Buhler and N. Giuseppone, *Soft Matter*, 2014, **10**, 2926–2937.
5. CrysAlisPro, Rigaku Oxford Diffraction Ltd., Yarnton (Oxfordshire, England), 2015.
6. Sheldrick, G. M., SHELXT - Integrated space-group and crystal-structure determination, *Acta Crystallogr., Sect. A: Found. Adv.*, 2015, **71**, 3–8.
7. Sheldrick, G. M., Crystal structure refinement with SHELXL, *Acta Crystallogr., Sect. C: Struct. Chem.*, 2015, **71**, 3–8.
8. J. M. Alaranta, K.-N. Truong, M. F. Matus, S. A. Malola, K. T. Rissanen, S. S. Shroff, V. S. Marjomäki, H. J. Häkkinen and T. M. Lahtinen, *Dyes and Pigments*, 2022, **208**.
9. Y. Zhao, D. G. Truhlar, *Theor. Chem. Acc.* 2008, **120**, 215–241.
10. S. K. P. E. Deppmeier, B. J. Driessen, A. J. Hehre, W. J. Hehre, T. S. Johnson, J. A. Ohlinger, “Spartan 20, build 1.1.5, Wavefunction Inc., 2022”.
11. X. Zhang, J. M. Herbert, *J. Phys. Chem. B* 2014, **118**, 7806–7817.
12. A. W. Lange, J. M. Herbert, *Chem. Phys. Lett.* 2011, **509**, 77–87.
13. J. D. McGhee and P. H. von Hippel, *J. Mol. Biol.*, 1974, **86**, 469–489